ALEPH 94-115
PHYSIC 94-100
F. Fidecaro et al.
11.07.1994

Measurement of the τ Lepton Lifetime with the Impact Parameter Sum method, using the 1992 ALEPH data sample

(preliminary result for summer conferences)

F. Fidecaro, A. Lusiani, A. Messineo, A. Sciabà

Abstract

The technique of the sum of the impact parameters (IPS) is used to measure the τ mean lifetime, from events where both τ leptons decay in one charged prong in the 1992 data sample. With respect to the last published analysis on the 1991 data sample, an improved τ selection (based on the new ALEPH standard τ selection) increases the purity and the efficiency. Additionally, work has been done to measure the impact parameter resolution with real data events: now the differences between muons and electrons are accounted for, and non gaussian tails are included in the maximum likelihood fit. 10464 τ candidates are selected from the 1992 ALEPH data sample, and a preliminary value of the lifetime has been obtained: $\tau_\tau = 295.0 \pm 3.9 \pm 4.4$ fs.

1 Introduction

At LEP the high purity and the size of the τ sample provide favourable experimental conditions for the mean lifetime measurement. This analysis takes advantage from the remarkable resolution achieved on the impact parameter (i.p.) measurement, due to the reduced multiple scattering contribution of high momentum τ decay products at LEP, and thanks to the precision of the ALEPH silicon strip vertex detector (VDET).

The τ lifetime is measured following the Impact Parameter Sum (IPS) technique, which is based on the measurement of the distance between tracks at the production point in events where both τ leptons decay in one charged prong. The IPS method was introduced in a previous note [1] and has been used to measure the τ lifetime for the 1991 data sample, in the latest measurement published by ALEPH [2]. The main features of the IPS technique are included in the following.

A new selection procedure is used to extract the 1992 τ sample, exploiting the most recent ALEPH standard τ selection, TSLT01 [3]. The efficiency has improved and the background contamination has been reduced.

The selection of the 1–1 topology decays is now the same as for the Impact Parameter Difference (IPD) analysis and has been provided by Wasserbaech [4]. It is now considered to be the standard selection for lifetime analyses using 1–1 topology τ events. With respect to our last analysis, the efficiency has improved, the background contamination is lower, and there is a better rejection of the $e^{\pm}$ tracks with hard Bremsstrahlung.

The increased statistics of the 1992 data and Monte Carlo τ event samples has revealed the presence of sizeable and extended non gaussian tails on the i.p. measurement error. The IPS analysis has been therefore upgraded to include a better estimate of the i.p. error distribution in the maximum likelihood fit. Furthermore, in order to estimate the corresponding systematic error, special care has been devoted to reliably estimate the Monte Carlo accuracy on the simulation of the resolution tails. To this aim $Z^0 \rightarrow q\bar{q}$ events are now used.

The present status of the analysis allows us to produce a preliminary measurement of the τ lifetime. In the following the IPS method will be summarized, the τ event sample will be described, updates and improvements to the last published IPS analysis (on the 1991 ALEPH data set) will be presented.

2 The Data Sample

The data sample used in this analysis was collected by ALEPH in 1992 at a center-of-mass energy of 91.27 GeV. MINI-DST's are used. The selection of good runs has been done by Wasserbaech [4] and is the intersection of the ALEPH official "Physics Groups" selections "VDET", "Heavy Flavor ECAL", and "Heavy Flavor HCAL" (from SCANBOOK), with the additional rejection of 17 runs having problems which are particularly serious for the τ lifetime measurement.

1235 good runs are selected, for an integrated luminosity of $25.1\,\mathrm{pb}^{-1}$, corresponding to $6.60 \cdot 10^5$ hadronic events or $3.21 \cdot 10^4$ produced τ pairs. The calculation of these numbers is explained in [4]. This sample is 2.7 times bigger than that used in the published analysis of the 1991 data.

Table 1: Number of Monte Carlo events for the samples used in this analysis. The corresponding expected figures are also quoted for the 1992 ALEPH data sample.

event type	Monte Carlo	1992 ALEPH data
$Z^0 \to \tau^+\tau^-$	297754	32144
$Z^0 \to \mu^+\mu^-$	50000	31681
$e^+e^- \to e^+e^-$	70000	69226
$Z^0 \to q\bar{q}$	1904490	659919
$\gamma\gamma \to \tau^+\tau^-(W > 4\,GeV/c^2)$	20000	5229
$\gamma\gamma \to \mu^+\mu^-(W > 2\,GeV/c^2)$	80000	74306
$\gamma\gamma \to e^+e^-(W > 4\,GeV/c^2)$	150000	44020
$\gamma\gamma \to q\bar{q}$ (QPM/ud)	12000	9844
$\gamma\gamma \to q\bar{q}$ (QPM/s)	1000	483
$\gamma\gamma \to q\bar{q}$ (QPM/c)	4000	3445
$\gamma\gamma \to q\bar{q}$ (VDM)	159200	142000

3 The Monte Carlo Samples

The $Z^0 \to \tau^+\tau^-$ Monte Carlo used in this analysis sample contains 297754 events. Like for the real data, MINI-DST's are used. It has been generated with the KORL06 generator, with an input τ mass of $1776.9\,MeV/c^2$ and an input lifetime of 296 fs. The detector simulation was accomplished by GALEPH 255.01, the reconstruction by JULIA 271.07. At the moment, this is the last official ALEPH Monte Carlo production for the 1992 detector geometry.

Background studies use several other Monte Carlo samples, which are listed in table 1. All belong to the same production as the τ sample, with the exception of the $\gamma\gamma \to e^+e^-$ Monte Carlo event sample, which comes from the previous production (GALEPH 253, JULIA 264). This particular sample is not yet available in the last Monte Carlo production.

The $e^+e^- \to e^+e^-$ events were generated with UNIBAB, which improves the treatment of high order QED corrections in comparison with BABAMC, the previously used Monte Carlo generator. In particular, UNIBAB generates doubly radiative Bhabha events, which were not produced by BABAMC, and are an important source of background contamination in the 1–1 τ selection.

4 IPS analysis outline

For a τ decaying into a single charged particle one can in principle determine the decay length from the decay angle and the i.p. of the track with respect to the production point. In practice, however, if one considers a single $Z^0 \to \tau^+\tau^-$ event in e^+e^- collisions, this procedure is not applicable: the production point is only known within the beam envelope, and the τ direction cannot be precisely measured because of the undetected neutrinos in the τ decay.

The sum of the two impact parameters is not affected by the beam size smearing (in first approximation): it is therefore measured with high accuracy, thanks to the precision of the ALEPH vertex detector. The two i.p.'s are signed according to the following convention: the i.p. is positive if the particle moves counterclockwise in the $r - \varphi$ plane with respect to the

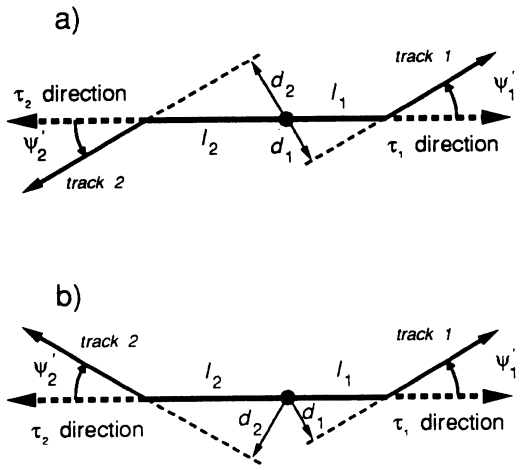

Figure 1: decays with 1–1 topology: a) $\psi_1' > 0$, $\psi_2' > 0$; b) $\psi_1' > 0$, $\psi_2' < 0$. The positive z-axis points out of the page. Angles are measured counterclockwise.

beam axis when at minimum distance, negative otherwise. Then $\delta' = d_1 + d_2$ does not depend on the Z production point (see fig. 1). This is strictly true only if the tracks are collinear, otherwise a contribution proportional to their acollinearity and to the beam size appears.

The event sphericity axis, computed with charged and neutral particles, is used to estimate the τ direction. For a fixed pair of decay angles (ψ_1', ψ_2'), each d_i has an exponential distribution with average $< d_i >= \ell \sin\vartheta \sin\psi_i'$, where ℓ is the mean decay length and ϑ is the τ polar angle. The distribution of δ' is a linear combination of these two exponential functions, that depends on the sign of δ' and the relative signs of the decay angles ψ_1' and ψ_2'. A maximum likelihood fit for ℓ is then performed, accounting for the measurement errors on δ' and $\psi_{1,2}'$.

4.1 The Likelihood Function

For the configuration shown in fig. 1a, where the true angles are positive ($\psi_1' > 0$,$\psi_2' > 0$), the distribution of the true sum of impact parameters δ' is given by:

$$\frac{dN}{d\delta'} = \begin{cases} \dfrac{\exp(-\delta'/\ell \sin\vartheta \sin\psi_1') - \exp(-\delta'/\ell \sin\vartheta \sin\psi_2')}{\ell \sin\vartheta(\sin\psi_1' - \sin\psi_2')} & \delta' > 0 \\ 0 & \delta' < 0 \end{cases} \tag{1}$$

This is obtained by folding the exponentials for d_1 and d_2, imposing $\delta' = d_1 + d_2$. On the other hand if $\psi_1' > 0$, $\psi_2' < 0$ as in fig. 1b, the distribution is:

$$\frac{dN}{d\delta'} = \begin{cases} \dfrac{\exp(-\delta'/\ell \sin\vartheta \sin\psi_1')}{\ell \sin\vartheta(\sin\psi_1' - \sin\psi_2')} & \delta' > 0 \\ \dfrac{\exp(\delta'/\ell \sin\vartheta \sin\psi_2')}{\ell \sin\vartheta(\sin\psi_1' - \sin\psi_2')} & \delta' < 0 \end{cases} \tag{2}$$

The expectation value of the distributions in eqs. 1 and 2 is always:

$$\left\langle \frac{dN}{d\delta'} \right\rangle = \ell \sin\vartheta \,(\sin\psi'_1 + \sin\psi'_2).$$

The distribution for the observed sum of impact parameters, is obtained by convolving the true δ' distribution with a resolution function for the three variables δ (the measured i.p. sum), ψ_1 and ψ_2 (the measured decay angles). Since the angular error contribution from tracking ($\simeq$ 0.5 mrad) is negligible with respect to the sphericity axis fluctuations due to the kinematics of the missing neutrinos ($\simeq$ 20 mrad), the resolution function can be can be written as two independent convolution functions g and h:

$$\frac{dN(\delta,\psi_1,\psi_2)}{d\delta} = \int d\psi'_1\, d\psi'_2\, h(\psi_1,\psi_2,\psi'_1,\psi'_2) \int d\delta'\, g(\delta,\delta') \frac{dN(\delta',\psi'_1,\psi'_2)}{d\delta'}. \tag{3}$$

The smearing on δ, described by g, is dominated by the resolution of the tracking devices, particularly VDET.

5 The Event Selection

Considerable improvements have been achieved on the event selection since the last published result on the 1991 ALEPH data set. A new selection of τ events has been provided and now there is a common selection used by all ALEPH analyses on one prong – one prong $Z^0 \to \tau^+\tau^-$ events.

The selection starts from the EDIR class 24, the extended leptonic selection. The logical condition SLUMOK.OR.LLUMOK=.TRUE. is required to insure that the detector and the trigger are operative, KEEVES=1 to skip events with online errors, XVDEOK=.TRUE. to select data where the silicon vertex detector was fully functional.

The τ pair candidates are selected by a modified version of TSLT01 [3,4], which provides better efficiency and much lower background contamination than SELTAU, the selection routine that was previously used. 25673 τ candidates survive. A further selection is applied to identify events where both τ leptons decay in a single charged prong (i.e. the 1–1 decay topology). This second selection procedure, named ONEONE, has been standardized by Wasserbaech and is described elsewhere [4]. Table 2 summarizes the effect of the ONEONE cuts, after which 10982 events are selected.

Furthermore, events are required to pass two additional cuts. The requirement $|\psi| < 0.15$ rad reduces the background from $\gamma\gamma$ processes further on; the requirement $|\delta| < 0.18$ cm removes some events on the tails, taking away some mismeasured ones. The cut on δ removes also a small number of events with large lifetime, thus affecting the mean lifetime fit. The effect is however rather moderate, and it is automatically corrected by the fact that the Monte Carlo fit is used as a calibration.

At the end of the selection 10464 events remain. This sample is 4.3 times bigger than the one selected from the 1991 ALEPH data set. The resulting impact parameter sum distribution is shown in fig. 2a. The solid histogram represents the τ Monte Carlo sample used in the analysis, normalized to the data: the points are the τ data, and the hatched histogram comes from a simulated zero-lifetime τ sample. The i.p. sum resolution from the Monte Carlo truth is 81 μm (R.M.S.), giving full access to the lifetime information. For comparison, the corresponding distribution for di-muons from Z^0 decays is shown in fig. 2b.

Table 2: surviving candidates for the 1–1 τ event selection.

Cut	MC	Data	$\varepsilon_{data}/\varepsilon_{mc}$
EDIR Class 24	100000	177731	
XLUMOK OR LLUMOK	100000	175958	
KEVEES	100000	175925	
XVDEOK	100000	175149	
TSLT01	78765	25673	
1–1 topology	45816	14806	0.991 ± 0.006
$\sum q = 0$	45211	14610	1.000 ± 0.001
Energy flow track	45180	14598	0.9999 ± 0.0002
Bhabha rejection	44644	14362	0.996 ± 0.001
less than 3 extra track	43300	13938	1.000 ± 0.001
$N_{VDET} \geq 1$	41324	13218	0.994 ± 0.002
$N^1_{ITC} \geq 4$	40469	12933	0.999 ± 0.002
$N_{TPC} \geq 8$	40326	12875	0.999 ± 0.001
χ^2/D.o.f. ≤ 5	40174	12484	0.974 ± 0.002
$p \geq 1.\,\mathrm{GeV/c}$	38828	12095	1.002 ± 0.002
Bremsstrahlung rejection	36551	11493	1.009 ± 0.002
Isolated γ rejection	34966	10982	0.9989 ± 0.002
$\lvert\psi\rvert < 0.15$ rad	33260	10475	1.003 ± 0.002
$\lvert\delta\rvert < 0.18\,\mathrm{cm}$	33237	10464	0.9996 ± 0.0003

5.1 Background studies

The background sample has been selected starting from the entire available Monte Carlo data set. The estimate of the background contamination after the TSLT01 τ selection has been investigated elsewhere [3]. The selection for the 1–1 decay topology removes additional background events; its acceptance for background events surviving TSLT01 has been measured with the Monte Carlo. At the end of the selection procedure we end-up with the background sample composition shown on the table 3.

6 Impact Parameter Sum Measurement Error

The i.p. sum δ is measured with a smearing whose distribution is accounted by $g(\delta, \delta')$. Such smearing is originated by the tracking errors and by the finite size of the interaction region.

The smearing due to the tracking errors is modelled by a sum of gaussians; the smearing due to the beam size is modelled as a further gaussian. A gaussian smearing applied on top of another gaussian smearing is equivalent to a single gaussian smearing with sigma equal to the quadratic sum of the sigmas. Therefore, the beam size smearing is easily accounted for by properly increasing the sigmas of the gaussians that model the tracking errors.

6.1 Tracking errors on the impact parameter

The size of the tracking error on the i.p. measurements is computed in the reconstruction process, using estimates for the detector coordinate resolution and for the multiple scatter-

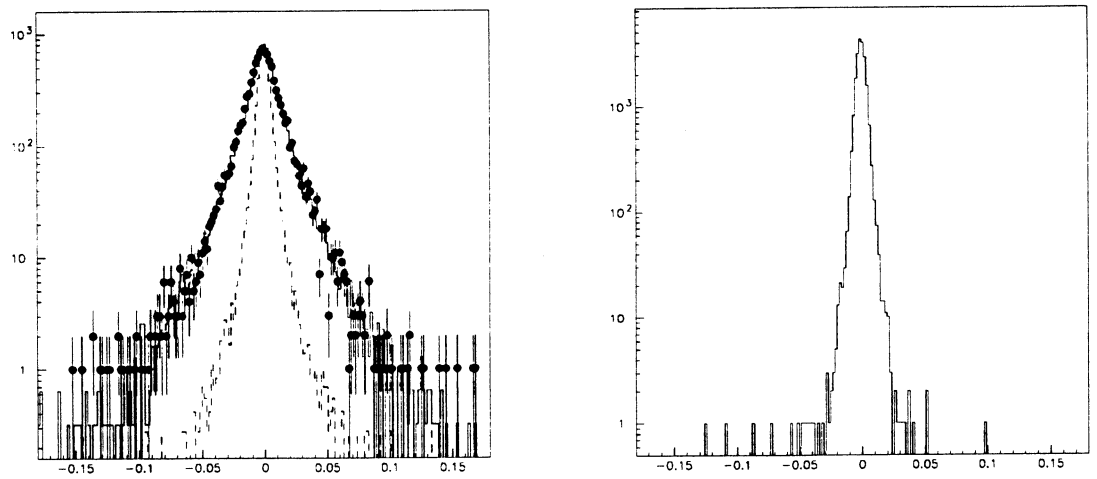

Figure 2: (a) distribution of the sum of impact parameters (δ) for tha τ Monte Carlo (continuous line), for real data data (points with error bars) and for simulated zero-lifetime τ pairs, using the Monte Carlo truth, (hatched line). (b) distribution of the sum of impact parameters δ for di-muon from Z decays in real data events.

ing. The reconstruction error serves as the sigma of a gaussian error distribution. This parametrization was used in the IPS analysis on the 1991 data sample.

Investigations on data and Monte Carlo clearly show that the tracking error distribution is not gaussian, and includes non gaussian tails that are sizeable and extended. Because of the improved statistical precision that is achievable with the 1992 τ data sample, it is desirable to correctly parametrize the i.p. resolution in the maximum likelihood fit, thus accounting for the non gaussian tails.

When looking at the i.p. resolution tails, one realizes also that they are substantially different for τ leptons decaying into muons, or electrons, or hadrons (see fig. 3). Muon tracks appear to have quite moderate non gaussian tails, electron tracks have more sizeable tails, and hadron tracks exhibit particularly wide tails. This is a related to the fact that very large measurement errors are caused by effects that depend on the particle type: Coulomb and strong detector interactions, decays in flight (e.g. $\pi^- \rightarrow \mu^- \overline{\nu}_\mu$) and electron Bremsstrahlung.

In the case of the electron τ decays, one can also see a statistically significant increase of the gaussian core sigma. Hadron decay tracks, on the other hand, appear to have a gaussian core that is statistically comparable to the muons.

In the following we describe how the i.p. sum resolution is computed, according to the following outline.

1. The gaussian resolution core is analysed with data and Monte Carlo samples for zero-lifetime events such as: $Z^0 \rightarrow \mu^+\mu^-$, $e^+e^- \rightarrow e^+e^-$, $\gamma\gamma \rightarrow \mu^+\mu^-$, $\gamma\gamma \rightarrow e^+e^-$. Appropriate correction coefficients are computed to correct the JULIA tracking error estimates in order to fit the gaussian core of the i.p. sum resolution for electrons and muons, both for data and Monte Carlo.

2. Electron and muon correction coefficients are combined according to the electron content

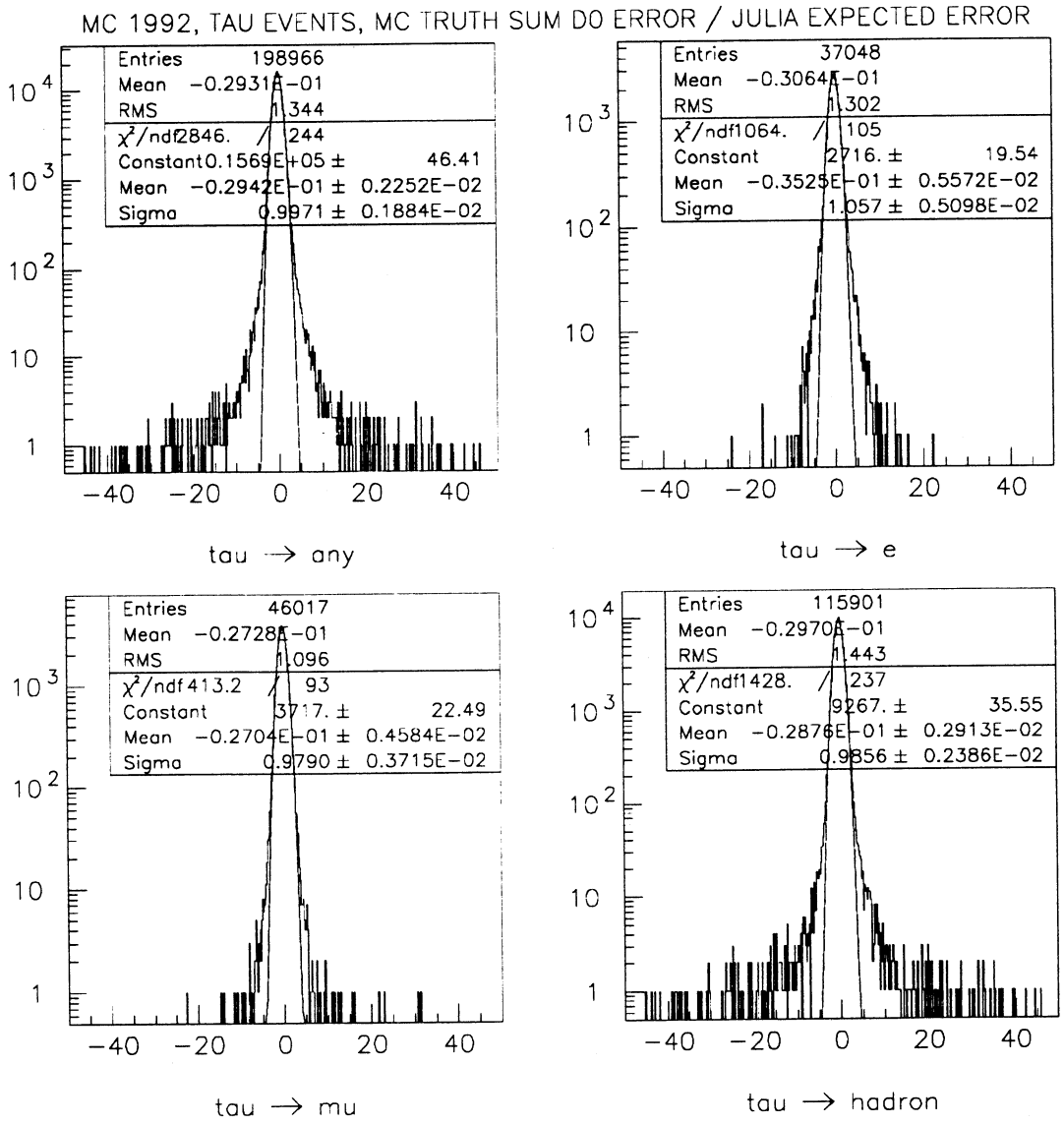

Figure 3: the four plots show the pull of the impact parameter measurement error from the τ Monte Carlo truth. The top left plot includes all τ decays, the other ones include respectively only muon, electron and hadron decays. The JULIA errors are tuned for τ leptons, by combining the electron and muon tuning coefficients according to the estimated electron content in the sample. Hadronic τ decays appear to behave like muons, for what concerns the gaussian core of the resolution. The gaussian fit of the pull distribution is close to width one, within the statistical uncertainty on the tuning coefficients.

Process	$\epsilon^{bkg.}_{1--1}(\%)$	background (%)	backgrounds events
e^+e^-	5.1 ± 1.3	0.034 ± 0.011	9 ± 3
$\mu^+\mu^-$	18.2 ± 3.4	0.049 ± 0.009	13 ± 4
$q\bar{q}$	2.3 ± 2.3	0.0058 ± 0.0058	1 ± 1
$\gamma\gamma \to e^+e^-$	43.8 ± 5.1	0.0526 ± 0.0075	14 ± 2
$\gamma\gamma \to \mu^+\mu^-$	44.9 ± 4.8	0.0539 ± 0.0073	14 ± 2
$\gamma\gamma \to \tau^+\tau^-$	28.6 ± 6.5	0.0140 ± 0.0038	4 ± 1
$\gamma\gamma \to q\bar{q}$	25 ± 18	0.0050 ± 0.0044	1 ± 1
cosmics	~ 9	~ 0.015	~ 4
total		0.229 ± 0.024	59 ± 6
selected events			10982

Table 3: Evaluation of the number of background events: the first column shows the efficiency of the 1–1 τ selection for background events selected by TSLT01; the second column shows the fraction of the background events with respect to the number of events selected by TSLT01; the third one shows the expected background for the sample of τ pairs selected from data.

in the selected data and Monte Carlo τ samples. Since hadrons appear to behave like muons in the τ Monte Carlo, hadronic τ decays are assumed to have the same gaussian resolution core as muon decays. With the resulting correction coefficients one expects that the core of the pull distribution (i.e. the distribution of the measurement error divided by its estimate) should be fitted by an unit width gaussian, for the selected τ samples that are used for the lifetime measurement.

3. The τ Monte Carlo pull distribution for all τ decays is fitted with three gaussians. The normalizations and the widths of the three gaussians are used to parametrize the shape of the distribution.

4. For the Monte Carlo τ sample, each event is given an impact parameter sum resolution composed by three gaussians: the gaussian core width is determined by the corrected JULIA tracking errors, and the other two gaussians widths and normalizations are fixed to reproduce the shape of the above pull distribution.

5. For the data τ sample, a symmetric procedure is followed for the gaussian core (that is tuned by means of data events). The tails relative to the gaussian core, however, are determined by the fit on the τ Monte Carlo pull distribution.

The deviation from symmetry in the last pass demands that the Monte Carlo be checked against real data to estimate the simulation accuracy for the non gaussian resolution tails. This is accomplished in the following way:

1. Again one exploits the zero-lifetime events such as: $Z^0 \to \mu^+\mu^-$, $e^+e^- \to e^+e^-$, $\gamma\gamma \to \mu^+\mu^-$, $\gamma\gamma \to e^+e^-$. The i.p. pull distributions are compared between data and Monte Carlo.

2. The i.p. resolution tails are particularly sizeable for hadronic τ decays. An estimate of the Monte Carlo simulation accuracy for this latter case is derived by analysing data

and Monte Carlo $Z^0 \to q\bar{q}$ events. The primary vertex is reconstructed and the negative side of the i.p. pull distribution is compared for data and Monte Carlo event samples.

6.2 Zero-lifetime event samples

The measurement error on the i.p. sum is experimentally accessible in real data events with zero-lifetime, such that: $Z^0 \to \mu^+\mu^-$, $e^+e^- \to e^+e^-$, $\gamma\gamma \to \mu^+\mu^-$, $\gamma\gamma \to e^+e^-$. All such events resemble the 1–1 topology of our τ sample: clean samples of such events can therefore be selected by a few appropriate modifications of the selection procedure used for 1–1 τ events. Since these events are used for resolution studies, they are selected starting from the same run selection as the τ sample. As for the τ data and Monte Carlo samples, MINI-DST's are used. Both data and Monte Carlo events undergo the same selection procedure in order to preserve a complete symmetry between them.

Special care has been devoted to avoid contamination of events with lifetime such as $Z^0 \to \tau^+\tau^-$ and $\gamma\gamma \to \tau^+\tau^-$: in all cases the background contamination has been investigated with Monte Carlo events and found negligible for the required level of precision.

6.2.1 $Z^0 \to \mu^+\mu^-$

In TSLT01 there are cuts to select τ leptons against muons: the sum of the charged energy for the two leading tracks is required to be less than 1.6 times the beam energy ($E_{\rm beam}$), and, if the event is "muon-like", the total reconstructed energy is required to be less than $1.8 \cdot E_{\rm beam}$. Bhabha events are eliminated by a suitable analysis of the measured energy depositions in the electromagnetic calorimeter (ECAL); a loose Bhabha identification is used for events with tracks close to ECAL cracks.

The TSLT01 cuts have been modified, such that muons are selected against τ leptons, by rejecting Bhabha-like events, and requiring that that the event is muon-like, and the total reconstructed energy is more than $1.8 \cdot E_{\rm beam}$. Finally, both leading tracks are required to be identified muons (in ALPHA, KMUIIF$>$ 10).

Muons are selected from the EDIR class 15, the leptonic selection. Since we use muons for resolution studies, background contamination from events with lifetime has been investigated, using the Monte Carlo. The only sizeable contamination comes from $Z^0 \to \tau^+\tau^-$ events. Subjecting the whole Monte Carlo sample of 297754 events to the muon selection, only 4 events survive. The estimated contamination in the 18426 di-muon candidates is 0.4 ± 0.2 events, which is negligible.

6.2.2 $e^+e^- \to e^+e^-$

In TSLT01 $e^+e^- \to e^+e^-$ events are recognized and cut by a loose electron selection plus a total energy cut above $1.6 \cdot E_{\rm beam}$. Such cuts are modified to select Bhabha events: a loose electron identification is required, the total energy and the sum of the charged energy for the two leading tracks is required to exceed $1.6 \cdot E_{\rm beam}$. The selection is then refined by requiring that both leading tracks are identified electrons in ALPHA (KEIDIP$=$ 1). Also Bhabha events are selected starting from the EDIR class 15.

The contamination coming from $Z^0 \to \tau^+\tau^-$ events has been investigated, using the τ Monte Carlo sample. The estimated contamination is 2 ± 0.5 events in 15093 candidates, which is negligible.

6.2.3 $\gamma\gamma \rightarrow \mu^+\mu^-$

$\gamma\gamma \rightarrow \mu^+\mu^-$ events are eliminated from the selected τ sample in TSLT01 by requiring, for the two leading tracks: either a sum of charged energy larger than $0.35 \cdot E_{\mathrm{beam}}$ or a transverse momentum mismatch larger than $0.066 \cdot E_{\mathrm{beam}}$. This condition is inverted.

A special Monte Carlo sample of $\gamma\gamma \rightarrow \mu^+\mu^-$ events has been generated for this analysis, with an event invariant mass cut at $W > 2\,\mathrm{GeV/c^2}$. To have a comparable momentum distribution in the data sample, one requires that the invariant mass of the event from the two leading tracks' momenta is above $2\,\mathrm{GeV/c^2}$ (both for data and Monte Carlo).

To select two muons in the final state the sum of fired planes in the hadronic calorimeter (HCAL) is required to be larger than or equal to 6. At this point, a number of cuts are applied to reduce the background coming from $Z^0 \rightarrow \tau^+\tau^-$. There must be exactly two tracks in the event. There can be at most one neutral energy flow object. Finally, one of the following conditions must hold:

- either $\cos(\vartheta_1 - \vartheta_2) > -0.98$,
- or $P_t(\mathrm{event}) < 0.02\sqrt{P_{t1}^2 + P_{t1}^2}$.

ϑ_1 and ϑ_2 are the polar angles of the two leading tracks, P_{t1} and P_{t2} the two transverse momenta, $P_t(\mathrm{event})$ is the module of the vector sum of the two transverse momenta. The first cut relies on the fact that $\gamma\gamma$ events have larger polar acollinearity than τ events, the second one relies on the fact that $\gamma\gamma \rightarrow \mu^+\mu^-$ events have no transverse momentum imbalance due to neutrinos in the final state. The resulting real data sample includes 1799 candidates, the Monte Carlo sample has 2044 events.

Investigations were done on sources of contamination from events with lifetime: according to Monte Carlo one expects a contamination of 3.9 ± 0.7 events from $Z^0 \rightarrow \tau^+\tau^-$ and 8 ± 1 events from $\gamma\gamma \rightarrow \tau^+\tau^-$.

Since the i.p. sum resolution depends on the particle type, as already discussed, contamination from events with electrons or hadrons in the final state has been investigated as well. Using Monte Carlo samples of $\gamma\gamma \rightarrow e^+e^-$ and $\gamma\gamma \rightarrow q\bar{q}$ events, it was found that no event survives the selection.

6.2.4 $\gamma\gamma \rightarrow e^+e^-$

$\gamma\gamma \rightarrow e^+e^-$ events are selected in the same way as $\gamma\gamma \rightarrow \mu^+\mu^-$, replacing the condition on the HCAL planes by the requirement that both leading tracks are identified as electrons in ALPHA (KEIDIP= 1).

In this case there is some asymmetry between data and Monte Carlo. The Monte Carlo sample comes from the last but one production for the 1992 detector geometry, and was produced with an event invariant mass cut at $W > 4\,\mathrm{GeV/c^2}$: 1356 events survive the selection cuts and, if the invariant mass of the event from the two leading tracks' momenta is required to be above $4\,\mathrm{GeV/c^2}$, 1307 events remain. The data sample, however, has a lower momentum spectrum: 1254 events survive all cuts and only 336 events survive the $4\,\mathrm{GeV/c^2}$ invariant mass cut.

It is therefore planned to generate a new Monte Carlo $\gamma\gamma \rightarrow e^+e^-$ sample with an event invariant mass cut at $W > 2\,\mathrm{GeV/c^2}$, and all parameters and software equal to the last official production for the 1992 ALEPH geometry. In the mean time, samples with different

momentum spectrum in data and Monte Carlo will be used, since there are too few real data events at high energy.

Background in the real data candidates has been again investigates by means on Monte Carlo. Among 1254 candidates one predicts 1.0 ± 0.3 $Z^0 \to \tau^+\tau^-$ events, 2.1 ± 0.7 $\gamma\gamma \to \tau^+\tau^-$ events, and no $\gamma\gamma \to \mu^+\mu^-$ and $\gamma\gamma \to q\bar{q}$ events.

It also deserves attention that both the data and Monte Carlo $\gamma\gamma \to e^+e^-$ MINI-DST's do not include the detailed ECAL information that is required for a Bremsstrahlung cut that is imposed for all other event samples that belong to the EDIR class 24 (see [4]). This cut aims at rejecting electron final states affected by hard Bremsstrahlung processes in the detector material, where a sizeable shift in the i.p. measurement is expected. The necessary information is only kept for events in the EDIR class 24, to which very few $\gamma\gamma \to e^+e^-$ events belong. This will be addressed in the later sections, when relevant.

6.3 $Z^0 \to q\bar{q}$ event sample for resolution studies

The selection for $Z^0 \to q\bar{q}$ events starts from the EDIR class 16. The QIPBTAG package[1] is executed to select good events, to reconstruct the primary vertex[2] and to compute the track impact parameters. QIPBTAG provides an event probability, based on the track impact parameters, that estimates how much likely is the hypothesis that all tracks come from the primary vertex, in the event under examination. This event probability is required to be larger than 0.1 in order to effectively remove events with lifetime, such as $Z^0 \to b\bar{b}$ and $Z^0 \to c\bar{c}$.

The QIPBTAG track selection is then used, which requires what follows. The track must have at least 4 TPC hits, and at least one $r\varphi$ and one z vertex detector coordinate in the same layer. The track must originate near the reconstructed primary vertex: $|d_0| < 0.5\,\mathrm{cm}$ and $|z_0| < 0.5\,\mathrm{cm}$. Errors on d_0 and z_0 must be less than 0.1 cm, and the χ^2/DOF of the track fit must be below 5. Tracks are then associated to their nearest jet. Tracks likely to have originated from photon conversions are also removed. A topological algorithm is used, which is described in [6].

Some further cuts are applied, on top of the QIPBTAG ones. Tracks are required to fail muon and electron identification in ALPHA (KEIDIP= 0 and KMUIIF< 5), since the interest is focused in hadrons.

QIPBTAG provides the impact parameter of the tracks with respect to the reconstructed primary vertex. The impact parameter is projected on to the $r\varphi$ plane, and the estimated error on the $r\varphi$ projection is computed as two terms: one due to the error matrix of the involved track, the second one due to the uncertainty on the primary vertex position. The term due to the primary vertex is required to be smaller than $25\,\mu\mathrm{m}$, to insure that it is not dominating the i.p. resolution.

6.4 Tuning the gaussian core of the resolution

This analysis requires that every track has at least one coordinate in one of the two layers of the vertex detector. Tracks within the acceptance of both VDET layers traverse an amount

[1] QIPBTAG is a package to tag b hadrons using track impact parameters, and is described elsewhere [6].

[2] The QIPBTAG package includes QFNDIP [7], a package that reconstructs the primary vertex for $Z^0 \to q\bar{q}$ events.

of material that is proportional to $1/\sin\vartheta$. The multiple scattering contribution to the i.p. resolution comes mainly from such material, and is proportional to the square root of the material thickness and on the extrapolation length, that goes like $1/\sin\vartheta$. Taking into account the momentum dependence, one can reasonably assume that measurement error on the i.p. (σ_{d0}) can be written as a superposition of two contributions:

$$\sigma_{d0}^2 = \sigma_0^2 + \sigma_{ms}^2/(p^2 \sin^3\vartheta) \tag{4}$$

where the first term accounts for the intrinsic detector resolution and the second one for the multiple scattering contribution. Following this assumption, the i.p. error that is computed in the track fit during reconstruction, σ_{ed0}, can be written in the same way:

$$\sigma_{ed0}^2 = \sigma_{e0}^2 + \sigma_{ems}^2/(p^2 \sin^3\vartheta) \tag{5}$$

The resolution parameters depend on the amount of vertex detector information that is available. The tracks can be grouped in three homogeneous subsets:

1. those with VDET $r\varphi$ hits on both layer;
2. those with VDET $r\varphi$ hits only on the inner layer;
3. those with VDET $r\varphi$ hits only on outer layer.

By fitting σ_{d0} and σ_{ed0} as functions of $p^2\sin^3\vartheta$, it becomes possible to extract the parameters σ_0, σ_{ms}, σ_{e0} and σ_{ems}, by means of which one can tune the estimated tracking errors such that they correctly reproduce the i.p. resolution that is derived from the data:

$${}^{(\text{tuned})}\sigma_{d0}^2 = \sigma_{ed0}^2 \cdot \frac{{}^{(\text{fit})}\sigma_0^2 + {}^{(\text{fit})}\sigma_{ms}^2/p^2\sin^3\vartheta}{{}^{(\text{fit})}\sigma_{e0}^2 + {}^{(\text{fit})}\sigma_{ems}^2/p^2\sin^3\vartheta} \tag{6}$$

Impact parameter measurement errors are experimentally accessible through the i.p. sum measurement for events with no lifetime content like $Z^0 \to \mu^+\mu^-$, $e^+e^- \to e^+e^-$, $\gamma\gamma \to \mu^+\mu^-$, $\gamma\gamma \to e^+e^-$.

In order to derive separate correction factors for the 3 different track subsets, it is convenient to organize the events in 3 classes:

1. both tracks with both layers;
2. one track with both layers, the other with no hit on the outer layer;
3. one track with both layers, the other with no hit on the inner layer, both tracks in the inner layer acceptance;

By fitting an i.p. sum distribution with a gaussian, one can obtain the gaussian sigma of the actual measurement error from the data themselves. Following eq. 4, this error can be written as:

$$\sigma_\delta^2 = \sigma_{1d0}^2 + \sigma_{2d0}^2 = \sigma_{10}^2 + \frac{\sigma_{1ms}^2}{p_1^2\sin^3\vartheta_1} + \sigma_{20}^2 + \frac{\sigma_{2ms}^2}{p_2^2\sin^3\vartheta_2} \tag{7}$$

It is useful to define an effective momentum P_{ms} for the whole event as:

$$\frac{1}{P_{ms}^2} = \frac{1}{p_1^2\sin^3\vartheta_1} + \frac{1}{p_2^2\sin^3\vartheta_2} \tag{8}$$

With this quantity:

$$\sigma_\delta^2 = (\sigma_{10}^2 + \sigma_{20}^2) + \frac{(\sigma_{1ms}^2 + \sigma_{2ms}^2)}{2P_{ms}^2} \cdot \frac{2(\sigma_{1ms}^2 p_2^2 \sin^3\vartheta_2 + \sigma_{2ms}^2 p_1^2 \sin^3\vartheta_1)}{(\sigma_{1ms}^2 + \sigma_{2ms}^2)(p_1^2 \sin^3\vartheta_1 + p_2^2 \sin^3\vartheta_2)} \tag{9}$$

For the first subset of events $\sigma_{1ms} = \sigma_{2ms} = {}^{bl}\sigma_{ms}$ and the last factor becomes:

$$\frac{2(\sigma_{1ms}^2 p_2^2 \sin^3\vartheta_2 + \sigma_{2ms}^2 p_1^2 \sin^3\vartheta_1)}{(\sigma_{1ms}^2 + \sigma_{2ms}^2)(p_1^2 \sin^3\vartheta_1 + p_2^2 \sin^3\vartheta_2)} = \frac{2 \cdot {}^{bl}\sigma_{ms}^2 (p_2^2 + p_1^2)}{(2 \cdot {}^{bl}\sigma_{ms}^2)(p_1^2 + p_2^2)} = 1 \tag{10}$$

The σ_{ms} parameters are not the same for the other two subsets, however by averaging in a P_{ms} bin one obtains:

$$\begin{aligned} &\left\langle \frac{2(\sigma_{1ms}^2 p_2^2 \sin^3\vartheta_2 + \sigma_{2ms}^2 p_1^2 \sin^3\vartheta_1)}{(\sigma_{1ms}^2 + \sigma_{2ms}^2)(p_1^2 \sin^3\vartheta_1 + p_2^2 \sin^3\vartheta_2)} \right\rangle = \\ &= 2\frac{\sigma_{1ms}^2 \left\langle \frac{p_2^2 \sin^3\vartheta_2}{p_1^2 \sin^3\vartheta_1 + p_2^2 \sin^3\vartheta_2} \right\rangle + \sigma_{2ms}^2 \left\langle \frac{p_1^2 \sin^3\vartheta_1}{p_1^2 \sin^3\vartheta_1 + p_2^2 \sin^3\vartheta_2} \right\rangle}{(\sigma_{1ms}^2 + \sigma_{2ms}^2)} \end{aligned} \tag{11}$$

The study of our event samples shows that:

$$\left\langle \frac{p_2^2 \sin^3\vartheta_2}{p_1^2 \sin^3\vartheta_1 + p_2^2 \sin^3\vartheta_2} \right\rangle \simeq \left\langle \frac{p_1^2 \sin^3\vartheta_1}{p_1^2 \sin^3\vartheta_1 + p_2^2 \sin^3\vartheta_2} \right\rangle \simeq 0.5 \tag{12}$$

within the statistical errors. Therefore, one can separately fit all three event subsets in P_{ms} bins according to:

$$\sigma_\delta^2 = (\sigma_{10}^2 + \sigma_{20}^2) + \frac{{}^{\text{class1}}\sigma_{ms}^2 + {}^{\text{class2}}\sigma_{ms}^2}{2P_{ms}^2} \tag{13}$$

and get the corresponding correction parameters to tune the estimated errors according to eq. 6.

At this point a further refinement is applied. The tuning coefficients that have been determined so far exploit most of the available events, but not all of them. In order to use also the remaining events, the same tuning method is applied a second time, on the tuned errors themselves. They are fitted, for all available events, in P_{ms} bins, and the same is done for the i.p. sum widths. In this way the coefficients for a second tuning correction are computed, with a slightly better accuracy.

The uncertainty on the tuning coefficients causes a systematic error on the τ lifetime measurement. There is evidence that the lifetime fit is not affected, in first approximation, by any change of the i.p. sum resolution that conserves the R.M.S. width. This is expected, since the lifetime fit, in first approximation, gets the τ lifetime by subtracting in quadrature the width of the resolution from the measured width of the i.p. sum distribution. As a consequence, the systematic error is mainly due to the uncertainty on the refined tuning coefficients (reported in table 4).

Figures 4, 5, 6, and 7 show the pull distributions for data and Monte Carlo zero lifetime event samples, with corrected and uncorrected estimated errors. When the proper tuning is applied, the gaussian fit sigmas are compatible with 1, if the statistical uncertainties are taken into account.

The final tuned errors are also checked for the Monte Carlo τ event sample, using the Monte Carlo truth to reconstruct the impact parameter sum measurement errors. A gaussian fit is

Table 4: precision of the parameters used to tune the impact parameter tracking errors, for muons and electrons.

	DATA		MC	
	$\frac{\Delta(\sigma_0/\sigma_{e0})}{\sigma_0/\sigma_{e0}}$	$\frac{\Delta(\sigma_{ms}/\sigma_{ems})}{\sigma_{ms}/\sigma_{ems}}$	$\frac{\Delta(\sigma_0/\sigma_{e0})}{\sigma_0/\sigma_{e0}}$	$\frac{\Delta(\sigma_{ms}/\sigma_{ems})}{\sigma_{ms}/\sigma_{ems}}$
muons	0.7%	2.9%	0.5%	2.5%
electrons	0.8%	4.0%	0.6%	3.0%

performed on the pull distributions for several event subsets in different momentum ranges and for different vertex detector topologies. The tuned errors show a satisfactory agreement with the goal of having unit width gaussian fits, within the expected statistical precision (see figures 3, 8, 9, 10 and 11).

As it has already pointed out (see section 6.2.4), the $\gamma\gamma \rightarrow e^+e^-$ MINI-DST's used in this analysis do not contain the detailed ECAL information that is required for a Bremsstrahlung cut that eliminates events were a sizeable i.p. measurement shift is expected. To a first approximation, this means that the non gaussian tails of the i.p. sum resolution are larger for $\gamma\gamma \rightarrow e^+e^-$ events than for kinematically comparable τ events. But since these events are fitted to get only the gaussian core of their resolution, only minor consequences are expected. This is confirmed by the fact that the gaussian fit to the pull distribution for τ leptons going into electrons is compatible with one, within the statistical accuracy given by the size of the $\gamma\gamma \rightarrow e^+e^-$ sample.

6.5 Parametrization of non gaussian tails

The pull distribution for the τ Monte Carlo sample (e.g. fig. 3) reveals non gaussian tails that extend up to 50 units. Investigations on the performance of the maximum likelihood fit for the τ lifetime have shown that events very far away on the resolution tails affect the fit result to a lesser degree with respect to events that are closer to the resolution core. A reasonable explanation is that events very far away from the resolution core do not simulate the presence of lifetime as well as closer events. With these observations in mind, we decided to fit the τ pull distribution with 3 gaussians, adjusting each one to fit a different region of the distribution.

The first gaussian fits the distribution core sigma, σ_g. The second gaussian has a sigma fixed to $3\sigma_g$ and its normalization is adjusted by requiring that the R.M.S. width of the first two gaussians reproduce σ_{10}, the R.M.S. width of the pull distribution truncated to $10\sigma_g$.

$$\sigma_{10}^2 = (1-a)\sigma_g^2 + a\sigma_2^2 \tag{14}$$

The third gaussian is adjusted such that the combination of the three gaussians reproduces the R.M.S. width of the whole pull distribution, σ. Within this constraint, the sigma and the normalization of the third gaussian are adjusted to fit the number of events observed beyond $10\sigma_g$.

The τ pull distribution D_{pull} will be:

$$D_{\text{pull}} = (1-b)((1-a)G_1(\sigma_g) + aG_2(3\sigma_g)) + bG_3(\sigma_b) \tag{15}$$

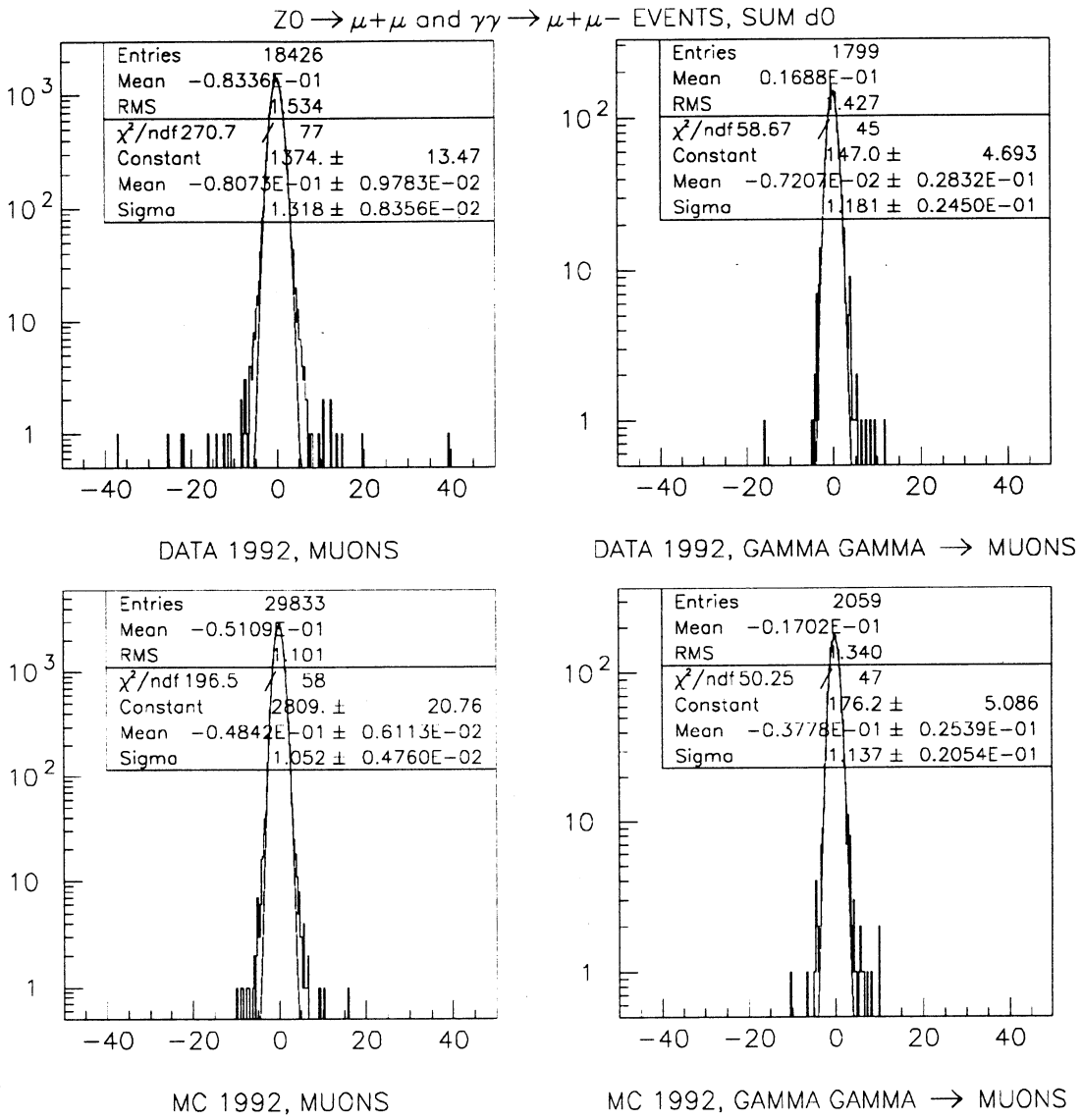

Figure 4: pull distributions for $Z^0 \to \mu^+\mu^-$ and $\gamma\gamma \to \mu^+\mu^-$ events, for data and Monte Carlo. The uncorrected JULIA errors are used, to show that they are often underestimated.

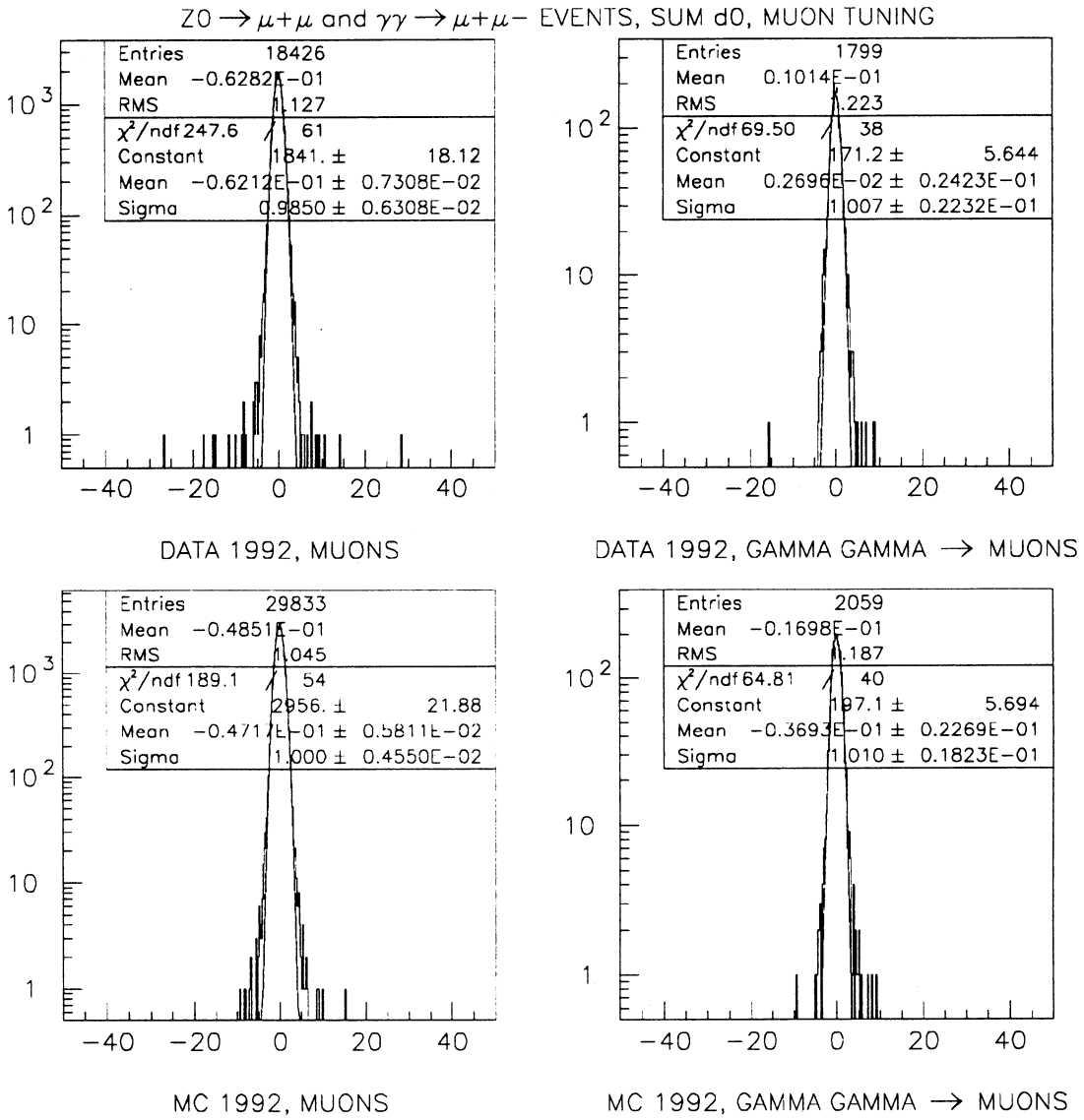

Figure 5: pull distributions for $Z^0 \to \mu^+\mu^-$ and $\gamma\gamma \to \mu^+\mu^-$ events, for data and Monte Carlo. The JULIA errors are tuned with these same events.

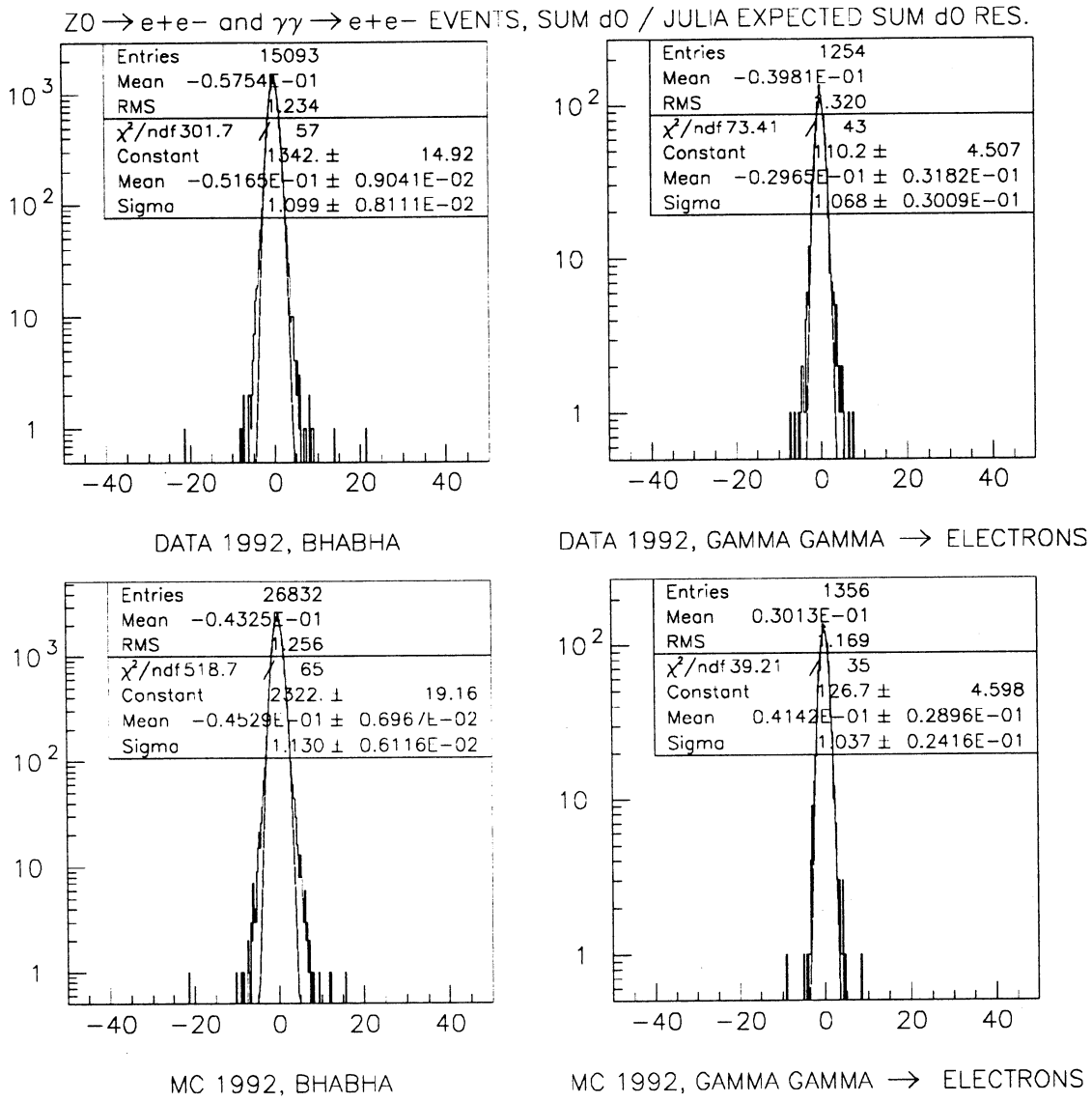

Figure 6: pull distributions for e^+e^- — e^+e^- and $\gamma\gamma$ — e^+e^- events, for data and Monte Carlo. The JULIA errors are tuned with the muon samples, and they seem underestimated.

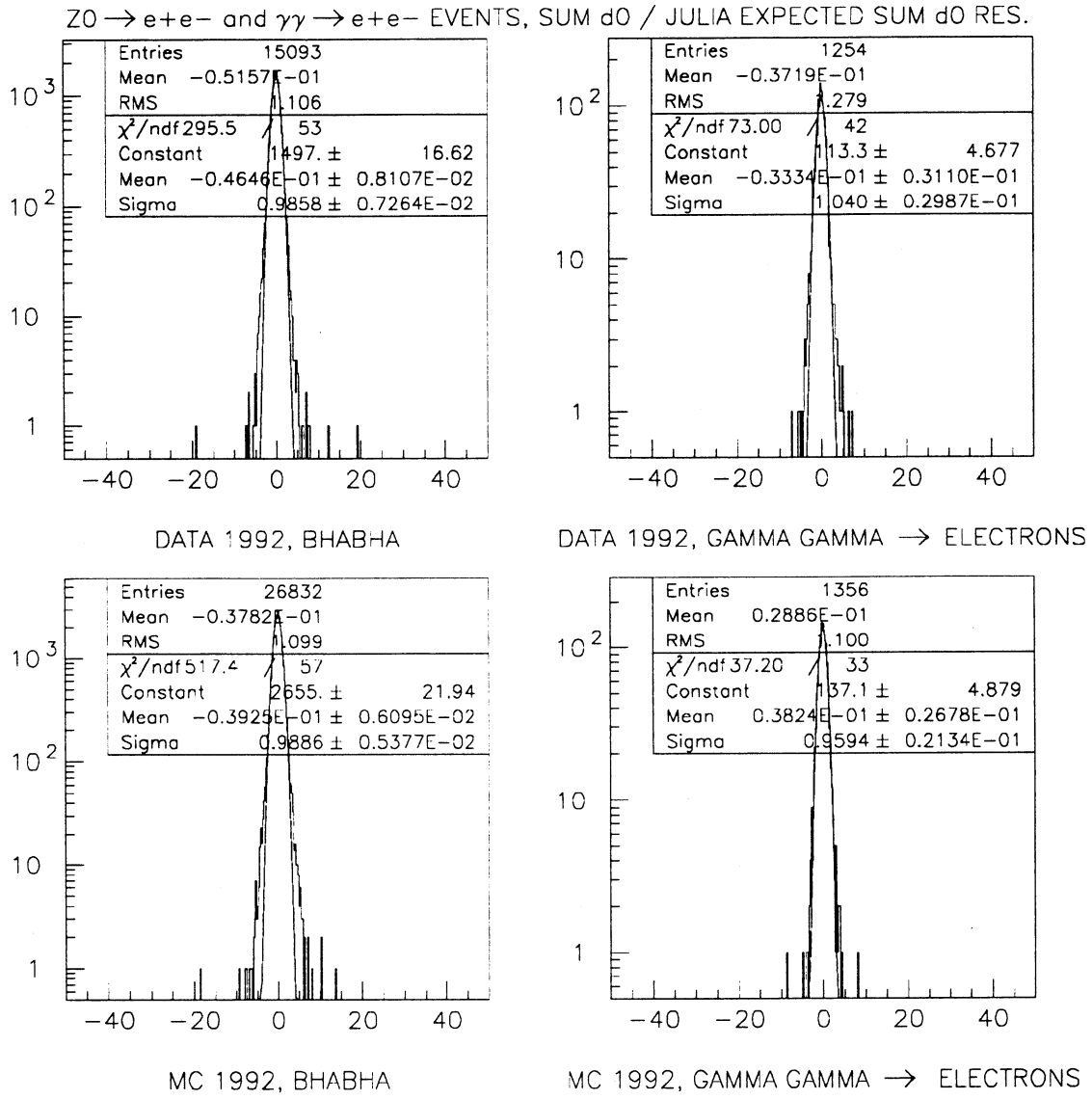

Figure 7: pull distributions for $e^+e^- \to e^+e^-$ and $\gamma\gamma \to e^+e^-$ events, for data and Monte Carlo. The JULIA errors are tuned with these same events.

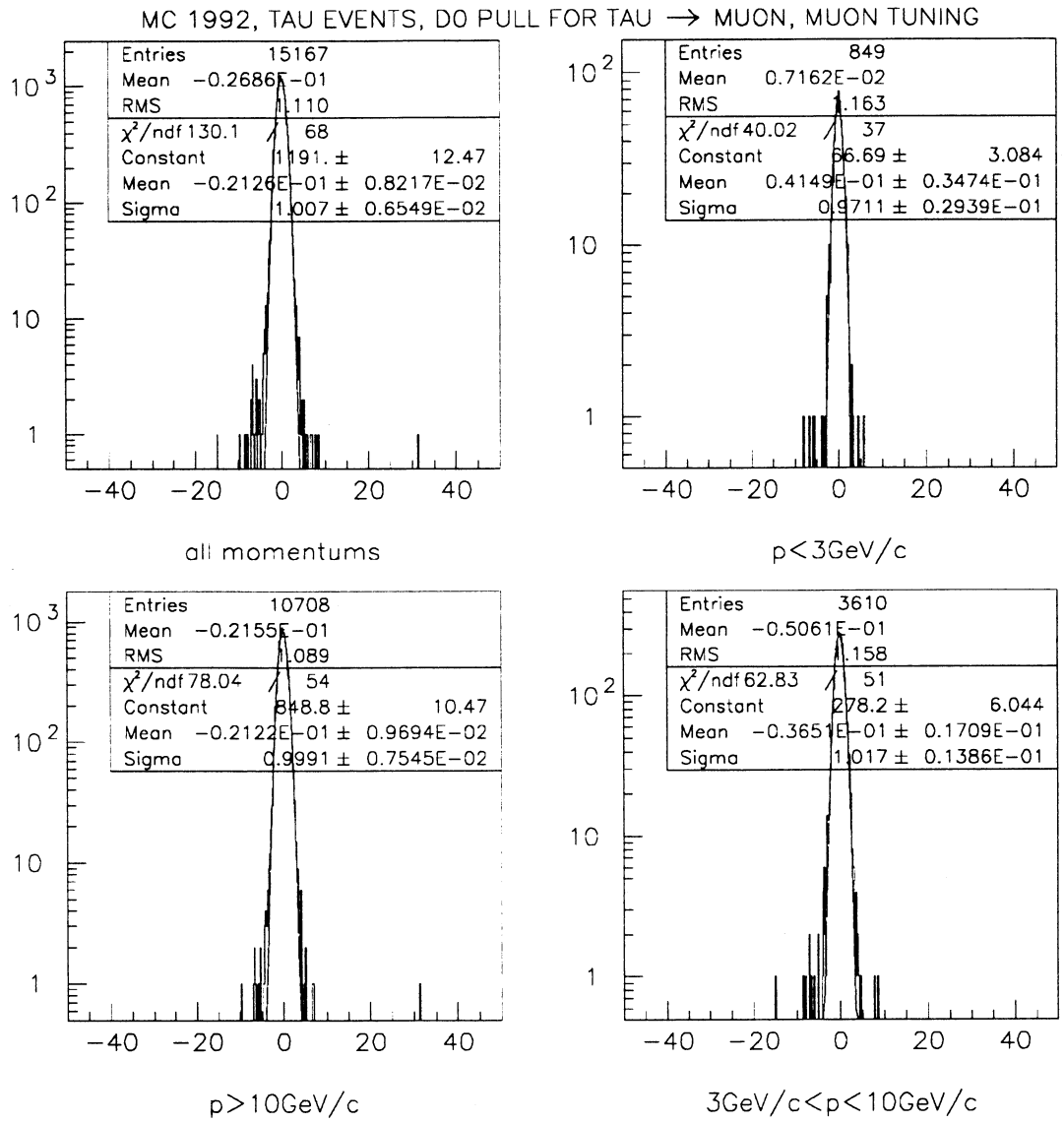

Figure 8: pull distributions for $Z^0 \rightarrow \tau^+\tau^-$ Monte Carlo events, where τ leptons decay into muons. Since these events have lifetime, the impact parameter measurement errors have been derived by using the Monte Carlo truth. By looking at low momentum events, the accuracy on the multiple scattering contribution to the i.p. resolution can be checked, by looking at the high momentum spectrum the detector intrinsic resolution term is verified. The JULIA errors are tuned for muons, and they look appropriate. To increase the statistics, the four histograms accumulate the pull for tracks, instead of events (where the branching ratio $\tau \rightarrow \mu$ would count twice).

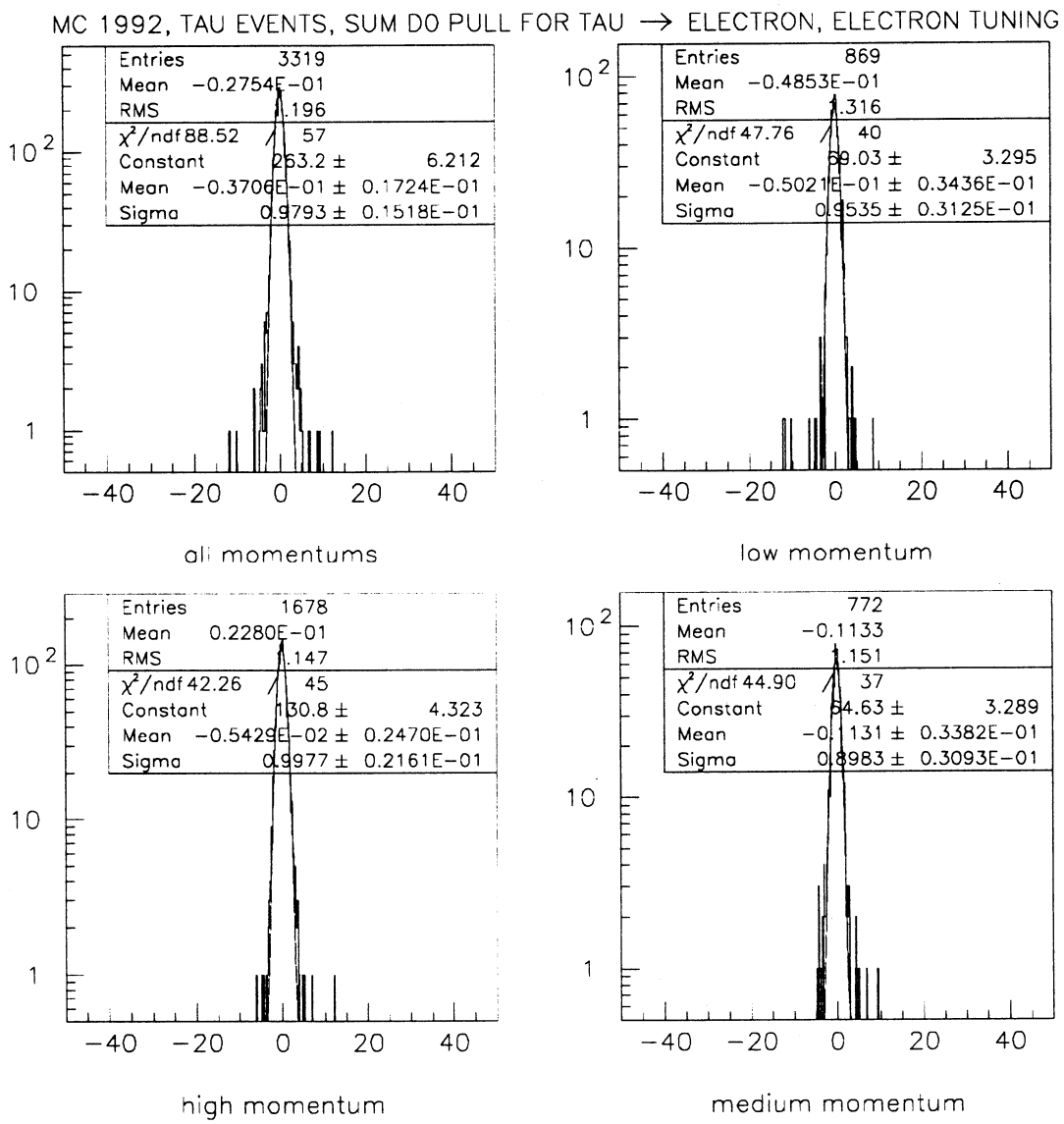

Figure 9: pull distributions for $Z^0 \rightarrow \tau^+\tau^-$ Monte Carlo events, where τ leptons decay into electrons. Since these events have lifetime, the impact parameter measurement errors have been derived by using the Monte Carlo truth. By looking at low momentum events, the accuracy on the multiple scattering contribution to the i.p. resolution can be checked, by looking at the high momentum spectrum the detector intrinsic resolution term is verified. The JULIA errors are tuned for electrons, and they look appropriate. The pull distribution uses the i.p. sum, since the Bremsstrahlung effect causes asymmetric error distributions for single tracks.

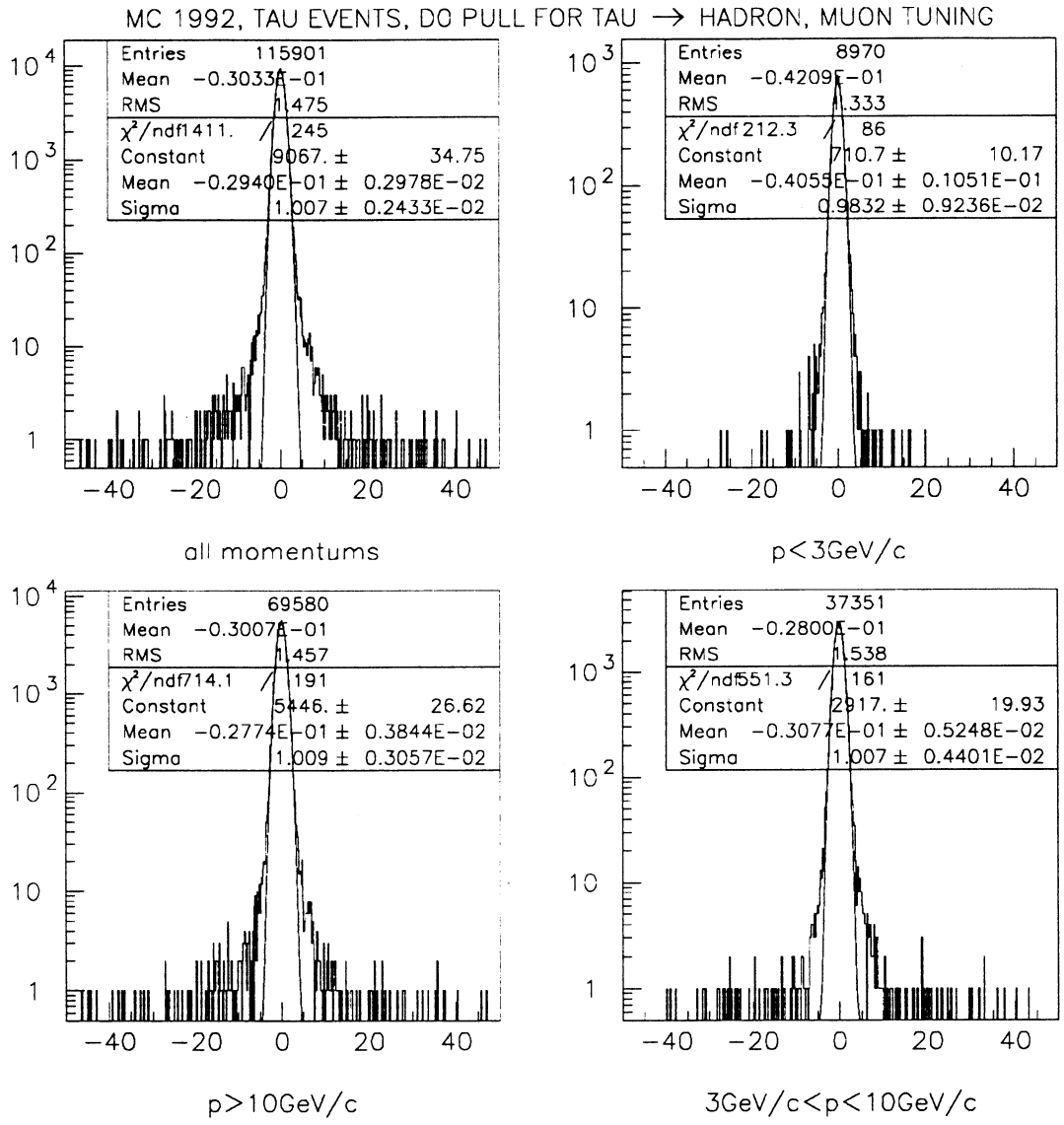

Figure 10: pull distributions for $Z^0 \rightarrow \tau^+\tau^-$ Monte Carlo events, where τ leptons decay into hadrons. Since these events have lifetime, the impact parameter measurement errors have been derived by using the Monte Carlo truth. By looking at low momentum events, the accuracy on the multiple scattering contribution to the i.p. resolution can be checked, by looking at the high momentum spectrum the detector intrinsic resolution term is verified. The JULIA errors are tuned for muons, and they look appropriate. Compared to muon decays, these events exhibit more sizeable ad more extended tails.

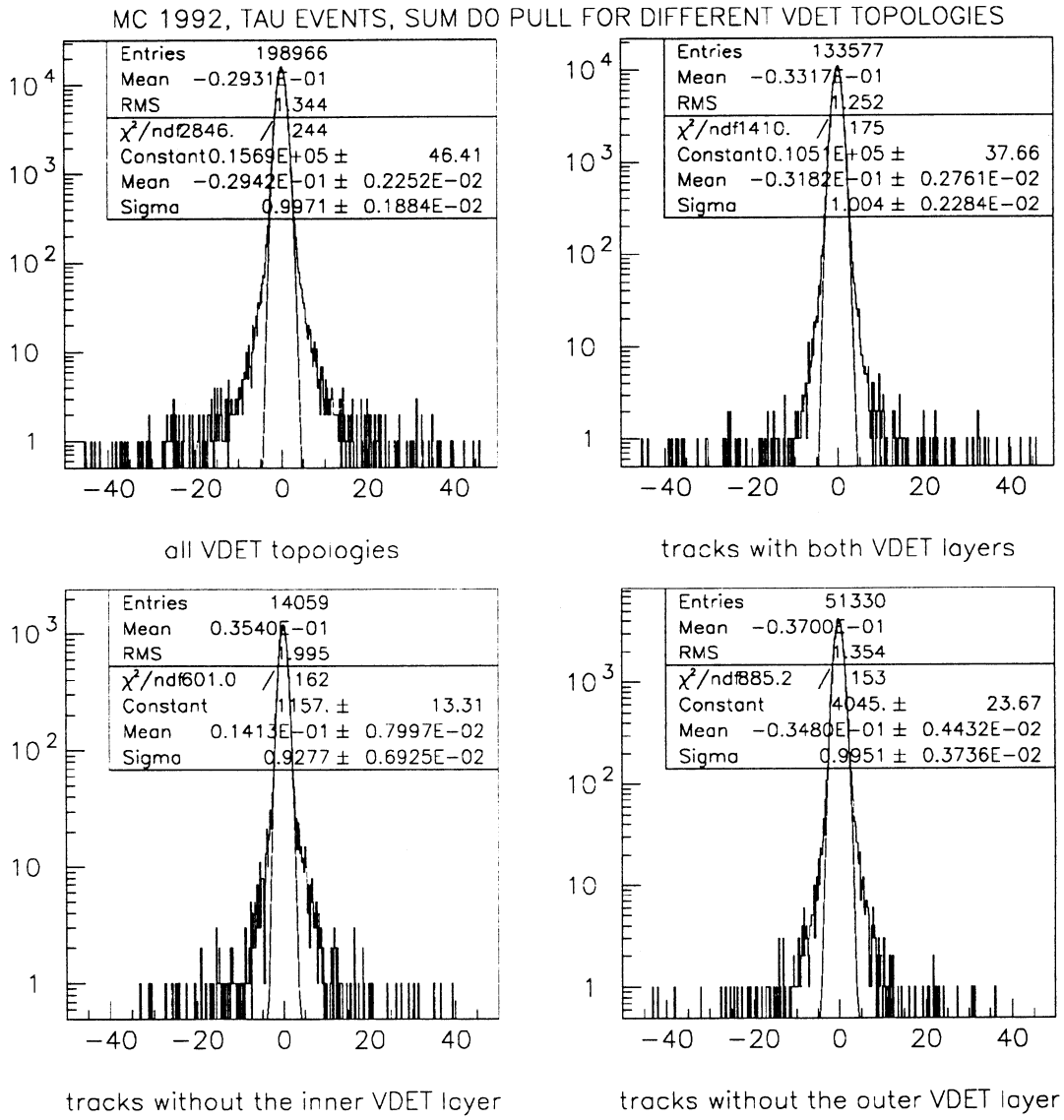

Figure 11: pull distributions for $Z^0 \to \tau^+\tau^-$ Monte Carlo events. Four sub-samples are shown, the first include all tracks, the second tracks that have hits on both the inner and outer VDET layer, the third tracks that have no hit on the inner layers, the fourth tracks that have no hit on the outer layer. Tracks without the inner layer exhibit the largest discrepancy, that should however be compared with the accuracy on the correction for this specific topology, which amounts to 3% for the detector intrinsic term, and 13.2% for the multiple scattering term.

where G_1, G_2 and G_3 are normalized gaussian distributions.

This parametrization is rather arbitrary, however it appears to fit the data quite well (see fig. 12). Additionally, each of the three gaussians fits the R.M.S. contribution of a different region of the pull distribution, and this makes it more straightforward to estimate the effect of the Monte Carlo simulation accuracy on the τ lifetime systematic error. This will be more evident in the following. Finally, the effect of changing the parametrization has been investigated: it is moderate, and it has been included in the systematic error.

The fit on the τ Monte Carlo pull distribution is used to get the *shape* of the non gaussian tails relative to the gaussian core, i.e. the parameters: a, b, σ_b/σ_g. Such parameters are used to describe the tails for the data and Monte Carlo i.p. resolution, once the core has been rendered by the JULIA errors after tuning.

Since the Monte Carlo non gaussian tails are used for the real data, it is important to check the simulation accuracy on the measurement errors: this is addressed in the following.

6.5.1 Simulation accuracy for "leptonic" resolution tails

As already noted, the amount of events on the non gaussian resolution tails is different between hadronic and leptonic τ decays. For electron and muon decays the resolution tails can be investigated by looking again at events with zero-lifetime, such as: $Z^0 \to \mu^+\mu^-$, $e^+e^- \to e^+e^-$, $\gamma\gamma \to \mu^+\mu^-$, $\gamma\gamma \to e^+e^-$.

In order to estimate the data – Monte Carlo discrepancies, the pull distribution is first fit to a gaussian, to get the gaussian core sigma σ_g. Then the following quantities are measured:

1. N_g, the number of events within $3\sigma_g$: this can be thought as an approximation of the number of events belonging to the gaussian core of the pull distribution;
2. N_{10}, the number of events within $10\sigma_g$;
3. σ_{10}, the R.M.S. width of the pull distribution truncated to $10\sigma_g$;
4. N, the total number of events in the distribution;
5. σ, the R.M.S. width of the whole distribution.

In order to concentrate on the shape of the pull distribution, the following derived quantities are computed, which are all normalized either to the total number of events in the distribution, or to the gaussian core sigma:

1. $\dfrac{N_{10} - N_g}{N}$, the percentage of events in the region between $3\sigma_g$ and $10\sigma_g$;
2. $\dfrac{\sigma_{10} - \sigma_g}{\sigma_g}$, the percentage of R.M.S. width contributed by events within $10\sigma_g$ and not contained in the gaussian core;
3. $\dfrac{N - N_{10}}{N}$, the percentage of events beyond $10\sigma_g$;
4. $\dfrac{\sigma - \sigma_{10}}{\sigma_g}$, the percentage of R.M.S. width contributed by events beyond $10\sigma_g$.

These last four quantities can be compared between data and Monte Carlo data samples, and describe the shape of the pull distribution tails relative to the gaussian core.

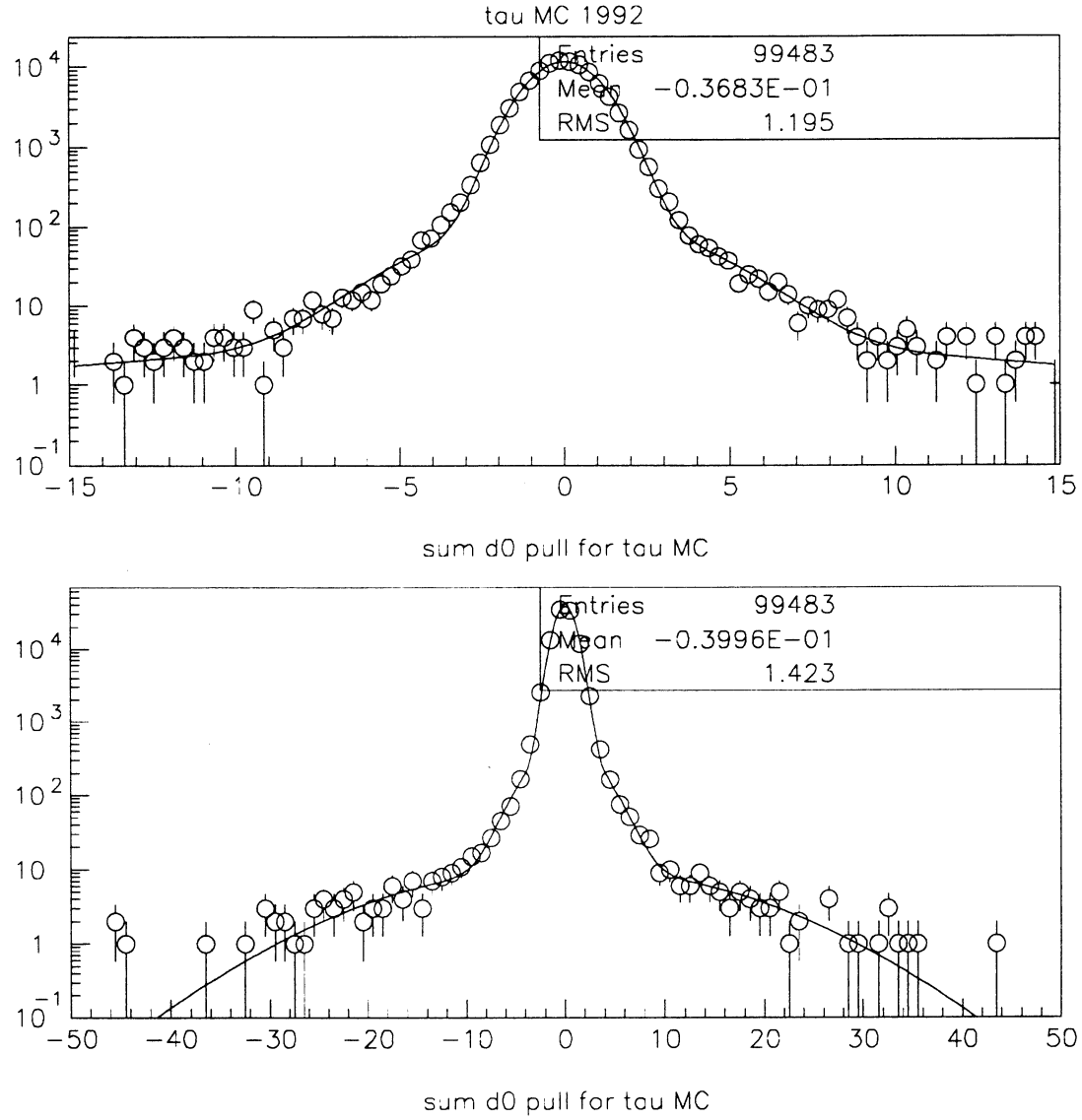

Figure 12: τ Monte Carlo i.p. sum measurement error distribution. The first plot shows a restricted range. A fit with three gaussians seems to match the distribution reasonably well.

6.5.2 Simulation accuracy for "hadronic" resolution tails

In order to investigate the i.p. resolution tails for hadrons, one uses tracks from $Z^0 \rightarrow q\bar{q}$ events, selected as described in section 6.3. As already mentioned, the QIPBTAG package is used to reconstruct the primary vertex and to compute the track impact parameters.

QIPBTAG assigns a positive sign to the i.p. if the track reaches the closest approach to its jet downstream with respect to the primary vertex, otherwise a negative sign is used. Tracks with lifetime have positive impact parameters, unless resolution is taken into account. The negative side of the i.p. distribution should therefore be only caused by the measurement resolution on tracks with no lifetime. Actually, the presence of measurements errors on the jet direction and on the tracking parameters causes a relatively small contamination of tracks which have lifetime but have measured negative impact parameters. Such contamination is at the level of a per cent after the QIPBTAG event probability cut against lifetime events that was used in this selection (see [6]).

The negative impact parameter significance, or pull, $-d/\sigma_d$ is used to compare data and Monte Carlo non gaussian tails. The track sample is then classified in 6 subsets according to the following properties:

- the VDET hits, that can be either 1 or 2;
- the momentum, that can be low (1..2 GeV/c), high (10..25 GeV/c) and medium (2..10 GeV/c); low momentum tracks are dominated by multiple scattering uncertainties, while high momentum tracks are affected mainly by detector measurement errors, alignment, material interactions.

For all these sub-samples, the tails are "measured" as already described for the lepton events. As one can see from fig. 13 and fig. 14, there is a fair agreement between data and Monte Carlo.

6.5.3 Estimate of the Monte Carlo simulation accuracy on tails

Tables 5 and 6 summarize the results on the data - Monte Carlo comparison on the i.p. pull distribution tails. Table 5 lists the R.M.S. contributions of events within 10 gaussian core sigmas σ_g, table 6 the contributions of events beyond $10\sigma_g$. The errors on the data - Monte Carlo discrepancies are computed from the number of events in the appropriate range. The relative error on the R.M.S. widths is taken to be $1/\sqrt{2N(\text{events})}$, the error expected for the R.M.S. of a sample distributed as a gaussian of width σ. Since events are actually confined in a restricted range, the statistical errors are overestimated.

As it has already pointed out (see section 6.2.4), the $\gamma\gamma \rightarrow e^+e^-$ MINI-DST's used in this analysis do not contain the detailed ECAL information that is required for a Bremsstrahlung cut that eliminates events were a sizeable i.p. measurement shift is expected. To a first approximation, this means that the non gaussian tails of the i.p. sum resolution are larger for $\gamma\gamma \rightarrow e^+e^-$ events than for comparable τ events. However, the same annotation applies symmetrically to data and Monte Carlo events, such that it is still sensible to compare them, in this regard.

For the same events it should also be noted that, *at this preliminary stage of the analysis*, the momentum spectrum is different between the data and the Monte Carlo spectrum (see section 6.2.4). This affects the comparisons in tables 5 and 6.

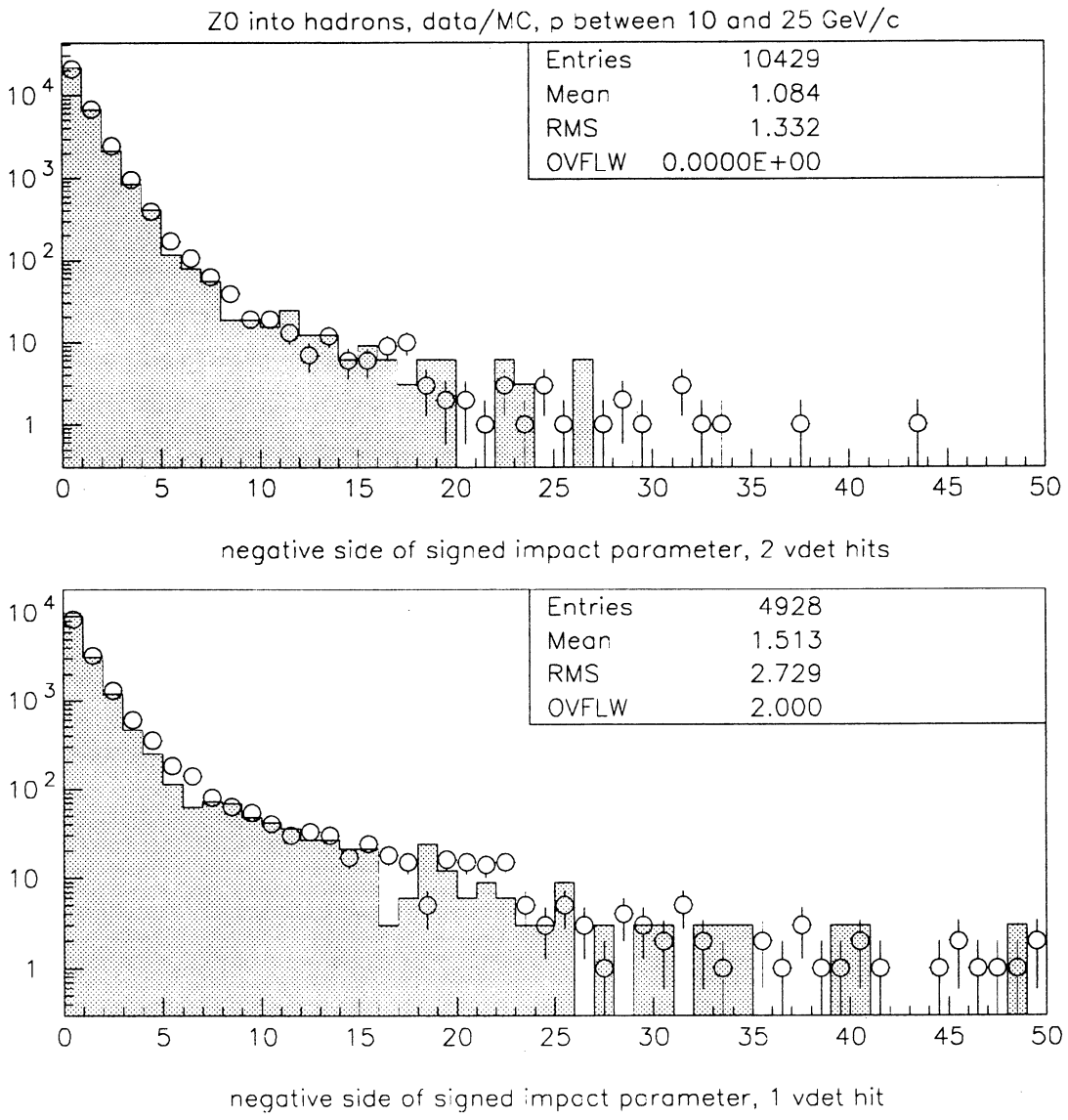

Figure 13: negative impact parameter significance compared between data and Monte Carlo. The plots show tracks with momentum between 10 and 25 GeV/c: tracks with two VDET hits enter the first plot, tracks with one VDET hit the second one.

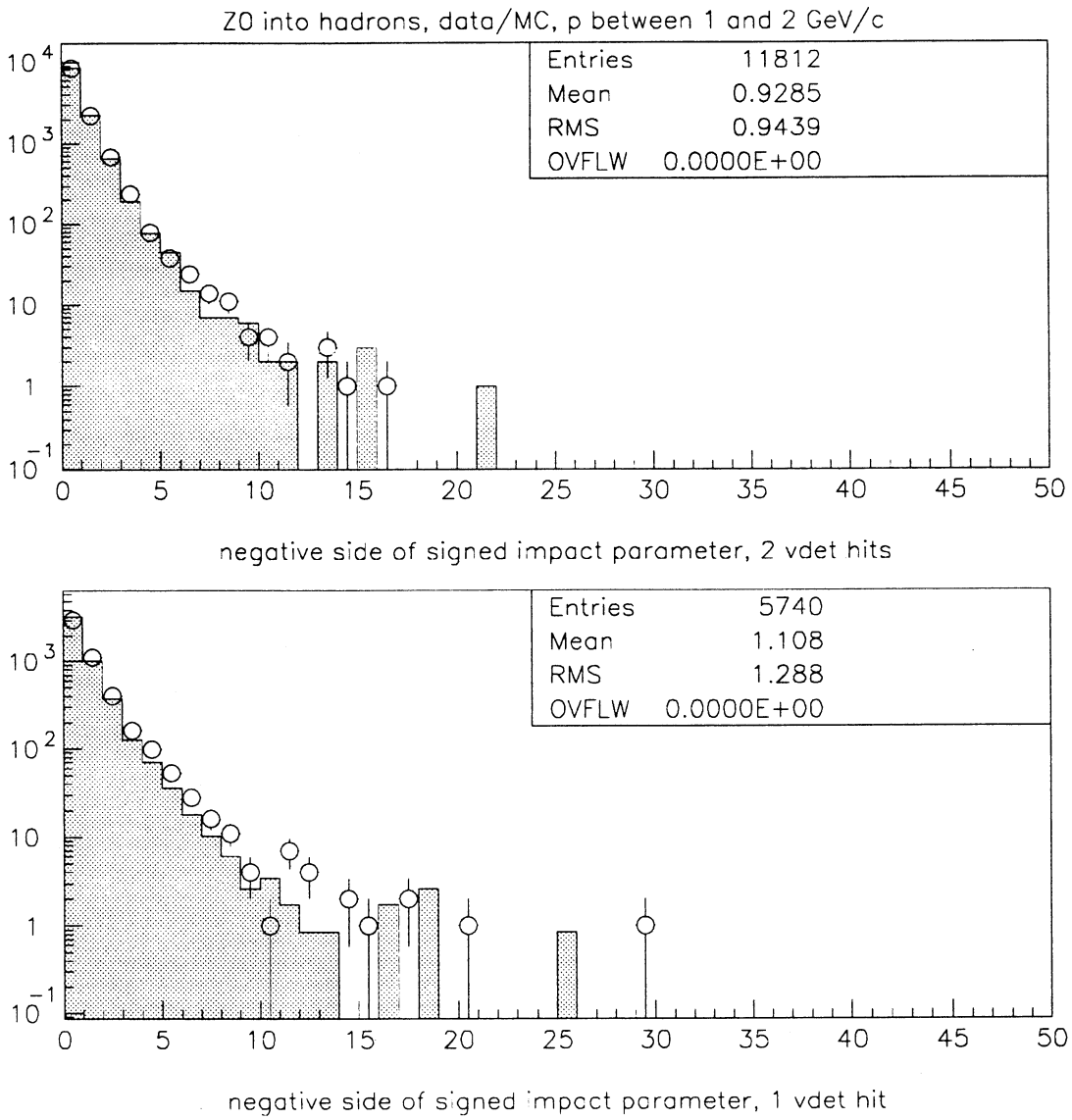

Figure 14: negative impact parameter significance compared between data and Monte Carlo. The plots show tracks with momentum between 1 and 2 GeV/c: tracks with two VDET hits enter the first plot, tracks with one VDET hit the second one.

$\frac{\sigma_{10}-\sigma_g}{\sigma_g}$ in % :	MC	data	Δ	$\sim\sigma(\Delta)$
$\gamma\gamma \to \mu^+\mu^-$	19.51%	18.18%	−1.33%	5.36%
$Z^0 \to \mu^+\mu^-$	4.47%	8.79%	4.32%	0.82%
$\gamma\gamma \to e^+e^-$	14.17%	26.56%	12.49%	6.66%
$e^+e^- \to e^+e^-$	11.01%	11.50%	0.50%	1.08%
$Z^0 \to q\bar{q}$, 2 VD hits, P in 10..25 GeV	35.70%	34.89%	−0.81%	2.36%
$Z^0 \to q\bar{q}$, 2 VD hits, P in 2..10 GeV	31.03%	34.45%	3.42%	1.97%
$Z^0 \to q\bar{q}$, 2 VD hits, P in 1..2 GeV	33.97%	35.15%	1.18%	2.75%
$Z^0 \to q\bar{q}$, 1 VD hit, P in 10..25 GeV	64.75%	69.11%	4.35%	4.93%
$Z^0 \to q\bar{q}$, 1 VD hit, P in 2..10 GeV	58.49%	63.51%	5.02%	4.10%
$Z^0 \to q\bar{q}$, 1 VD hit, P in 1..2 GeV	43.64%	46.54%	2.89%	4.56%

Table 5: impact parameter pull distribution tails within $10\sigma_g$: data – MC differences on the R.M.S. contributions relative to the gaussian sigma core and fair estimates of their statistical accuracies.

$\frac{\sigma-\sigma_{10}}{\sigma_g}$ in % :	MC	data	Δ	$\sim\sigma(\Delta)$
$\gamma\gamma \to \mu^+\mu^-$	0.00%	5.02%	5.02%	6.94%
$Z^0 \to \mu^+\mu^-$	0.34%	7.62%	7.28%	3.18%
$\gamma\gamma \to e^+e^-$	0.00%	0.00%	0.00%	*n.a.*
$e^+e^- \to e^+e^-$	1.42%	3.10%	1.68%	2.34%
$Z^0 \to q\bar{q}$, 2 VD hits, P in 10..25 GeV	27.74%	26.82%	−0.92%	6.90%
$Z^0 \to q\bar{q}$, 2 VD hits, P in 2..10 GeV	19.24%	20.38%	1.15%	6.13%
$Z^0 \to q\bar{q}$, 2 VD hits, P in 1..2 GeV	10.00%	7.27%	−2.73%	4.20%
$Z^0 \to q\bar{q}$, 1 VD hit, P in 10..25 GeV	105.90%	101.95%	−3.95%	15.72%
$Z^0 \to q\bar{q}$, 1 VD hit, P in 2..10 GeV	78.95%	60.64%	−18.31%	12.24%
$Z^0 \to q\bar{q}$, 1 VD hit, P in 1..2 GeV	14.96%	14.35%	−0.61%	8.43%

Table 6: impact parameter pull distribution tails beyond $10\sigma_g$: data – MC differences on the R.M.S. contributions relative to the gaussian sigma core and fair estimates of their statistical accuracies.

Concerning $Z^0 \to q\bar{q}$ events, it is worthwhile noting that, unlike for $Z^0 \to \tau^+\tau^-$ events, a considerable amount of tails in the i.p. measurement error are expected by pattern recognition errors and coordinate sharing. Both these phenomena increase at low momentum, and have more effect when the track has only 1 VDET coordinate. Hence high momentum tracks with 2 VDET coordinates are especially valuable to understand the simulation accuracy of the i.p. measurement errors for τ leptons: the small size of the corresponding discrepancies between real and simulated events is encouraging (see tables 5 and 6).

All considered, the data – Monte Carlo comparison shows that the Monte Carlo reproduces the resolution tails within $10\sigma_g$ at a level that can be fairly estimated at 4% of σ_g. For the tails beyond $10\sigma_g$, an educated guess of the simulation accuracy is $\sim 8\%$ of σ_g, or $\sim 30\%$ of the predicted R.M.S. contribution. These estimates will be used for the computation of the systematic error.

6.6 Beam size smearing on the impact parameter sum resolution

The impact parameter sum is smeared by tracking errors and by the finite size of the interaction region. This last effect contributes a gaussian smearing with variance:

$$\sigma_b^2 = 4\sin^2\frac{\Delta\varphi}{2}\left(\sigma_x^2\sin^2\overline{\varphi} + \sigma_y^2\cos^2\overline{\varphi}\right), \tag{16}$$

where σ_x and σ_y describe the beam size, $\overline{\varphi} = (\varphi_1+\varphi_2)/2$ is the average of the track azimuthal angles and $\Delta\varphi = \varphi_1 - \varphi_2 \pm \pi$ is the acollinearity of the tracks in the r-φ projection.

The tracking resolution affecting the i.p. sum is modelled with a sum of three gaussians. The beam size smearing can be accounted by replacing each one of the three gaussian sigmas by a value quadratically increased by σ_b.

However, *to obtain this preliminary result*, some shortcuts have been taken. The beam size effect has not been subtracted when fitting the i.p. sum resolution for zero-lifetime events. Consequently, the beam size smearing has not been applied in the maximum likelihood fit. The two effects compensate themselves, to some extent. To estimate the effect of this approximation, the beam size smearing has been computed for all the event samples that have been used for resolution studies. Table 7 lists the beam size contributions and the tracking resolution ones. For all event samples the beam size smearing represents less than a 0.5% contribution to the average tracking resolution. This is a very small effect, and we account for it in the systematic error, *for this preliminary result.*

7 The *h* function

In the measurement of the τ decay angles the original τ direction is approximated by the sphericity axis, computed from all the charged and neutral objects that are visible in the detector. As already seen in section 4.1, the h function describes the probability that the true decay angles are ψ_1' and ψ_2', while the measured ones are ψ_1 and ψ_2. The uncertainty on the measured decay angles is dominated by the kinematical effects caused by the undetected neutrinos in the computation of the sphericity axis, while tracking errors and other detector effects play a relatively minor role. Therefore, the h function can be numerically approximated by computing the sphericity axis on a large sample of τ pairs simulated at the kinematical level, without full detector simulation [2].

event sample	DATA		MC	
	$\sigma_b(\mu m)$	$\sigma_t(\mu m)$	$\sigma_b(\mu m)$	$\sigma_t(\mu m)$
$\gamma\gamma \to \mu^+\mu^-$	8.8	167	8.5	158
$Z^0 \to \mu^+\mu^-$	2.7	42	2.1	29
$\gamma\gamma \to e^+e^-$	8.5	192	11.5	122
$e^+e^- \to e^+e^-$	2.4	49	3.1	37
$Z^0 \to \tau^+\tau^-$	6.9	*n.a.*	6.7	69

Table 7: beam size smearing (σ_b) compared with tracking resolution R.M.S. width (σ_t) for the impact parameter sum of all relevant event samples.

The last published analysis used a h function that was appropriate for the SELTAU selection. Since a new τ selection is now used (TSLT01), the efficiency and the acceptance of the surviving candidates changed, and a new h function has been determined.

The functional parametrization of the h function is the same as the one used in the last published analysis [2]: thanks to the symmetry of the function with respect to an exchange between the two decay angles, we can use the simplified analytical form $h(S, S-S', D)$, where $S = \psi_1 + \psi_2$, $S' = \psi'_1 + \psi'_2$, and $D = \psi_1 - \psi_2$.

Improvements on the statistical precision have been obtained thanks to the increased size of the Monte Carlo sample, which includes now one million KORALZ τ pairs (without detector simulation). Using this event sample, the h function has been expressed by means of a numerical table, increasing the binning granularity for the three variables from (10,40,4) to (10,40,10).

The TSLT01 selection cuts were adapted to the available kinematical quantities: all the original cuts are used and they act only on the visible particles (neutrinos and tracks with momentum less then 200 MeV/c are not considered).

Simple geometrical acceptance cuts replace the requirements on the presence of the detector information. Where particle identification is needed, the Monte Carlo truth information is used. The accuracy of the selection procedure has been checked by comparing it to the TSLT01 τ selection acting on fully simulated Monte Carlo $\tau^+\tau^-$ events.

On Monte Carlo events with full detector simulation, the TSLT01 efficiency is (78.7±0.2)%. On the save events, using the Monte Carlo truth instead of the reconstructed quantities, the adapted TSLT01 is (80.4±0.2)% efficient. On the generator level events, the adapted selection has a slightly higher efficiency, (82.48 ± 0.04)%, as is expected by the fact that effects due to secondary interactions are not present in the Monte Carlo truth.

Fig. 15 shows that several relevant quantities used for the τ selection have comparable distributions for the fully reconstructed and the generator level τ pairs.

The selection for the 1–1 decay topology has been adapted to the generator level event sample as well. The request that tracks have at least one vertex detector hit has been transformed into a simple geometrical acceptance cut, neglecting the VDET inefficiency. The selection efficiencies for events with or without full detector simulation are listed in table 8.

When acting on fully simulated Monte Carlo events, the adapted selection is more efficient, since the requirements on the presence of detector coordinates have been replaced by

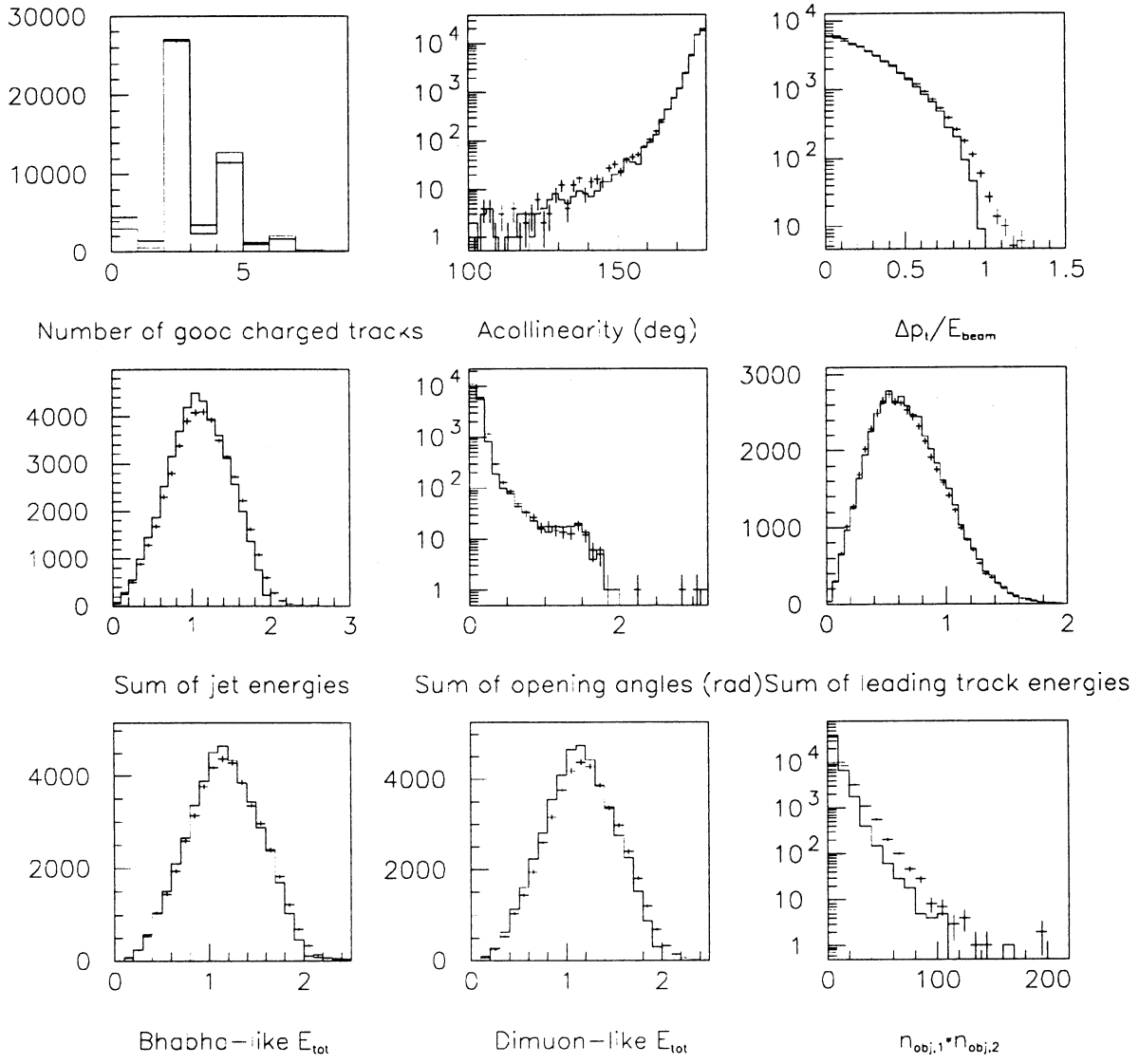

Figure 15: several quantities used in the τ selection are compared for the fully reconstructed and the generator level τ pairs, after selection.

selection	full detector simulation		no detector simulation
selection	ϵ	ϵ^*	ϵ
TSLT01+ONEONE	35.1 ± 0.2	37.3 ± 0.2	n.a.
adapted TSLT01+ONEONE	39.8 ± 0.2	38.2 ± 0.2	44.02 ± 0.05

Table 8: Selection efficiencies on $\tau^+\tau^-$ Monte Carlo events with and without full detector simulation; ϵ^* is the efficiency within the events that satisfy all the detector efficiency cuts that are not included in the adapted selection. The agreement increases. When no detector simulation has been performed, secondary interactions are missing, and therefore the efficiency is larger.

geometical acceptance cuts, neglecting any inefficiency. The adapted selection is closer if one compares the efficiencies on events that satisfy all the requirements regarding detector inefficiencies, (ϵ^*). The selection efficiency is considerably larger ($(44.02 \pm 0.05)\%$ for events without full detector simulation, since secondary interactions are missing. This affects the accuracy of the h function to the extent that different decay channels are affected in a different way. The effect has been checked and corrected for when considering the discrepancy of the electron fraction between data and Monte Carlo.

7.1 Fit Results on Monte Carlo and Data

The maximum likelihood fit to the τ data sample converges to a mean decay length $\ell = 0.2221 \pm 0.0029\,\mathrm{cm}$, for 10464 events. Accounting for the size of the fitted τ sample, the statistical error on the lifetime can be written as $1.34/\sqrt{N_\tau}$. Figures 16a–e show the distribution of δ divided in bins of $\psi_1 + \psi_2$ for the 1992 data. The fitted function is also shown.

The statistical error of the MINUIT fit has been compared with the R.M.S. spread of the results of 400 experiments performed on 400 sub-samples of the τ Monte Carlo. The two estimates are comparable.

The lifetime fit result is calibrated by using the Monte Carlo τ sample, where the input τ lifetime is 296 fs, the τ mass is $1776.9\,\mathrm{MeV/c^2}$, the center of mass energy is 91.27 GeV, and the radiative corrections to the τ momentum are included. The Monte Carlo fit result is $\ell = 0.2245 \pm 0.0009\,\mathrm{cm}$, while the sample has mean decay lenght $\ell = 0.2271\,\mathrm{cm}$, and mean lifetime $\tau_\tau = 296.8\,\mathrm{fs}$.

7.2 Systematic Biases and Uncertainties

Biases and systematic uncertainties on the lifetime fit result are expected to come from several sources. First, the maximum likelihood fit does not account for several details: the (modest) background, the charge dependent Bremsstrahlung effect on the i.p. measurement error for electrons, the transverse polarization correlation between the two τ leptons. Furthermore, the h function accuracy is limited by the binning, by the size of the Monte Carlo sample, by the effect of the approximate event selection used for the Monte Carlo sample, which lacks full detector simulation. Further systematic uncertainties arise from the parametrization and the tuning of the i.p. measurement errors, and from the related Monte Carlo simulation accuracy.

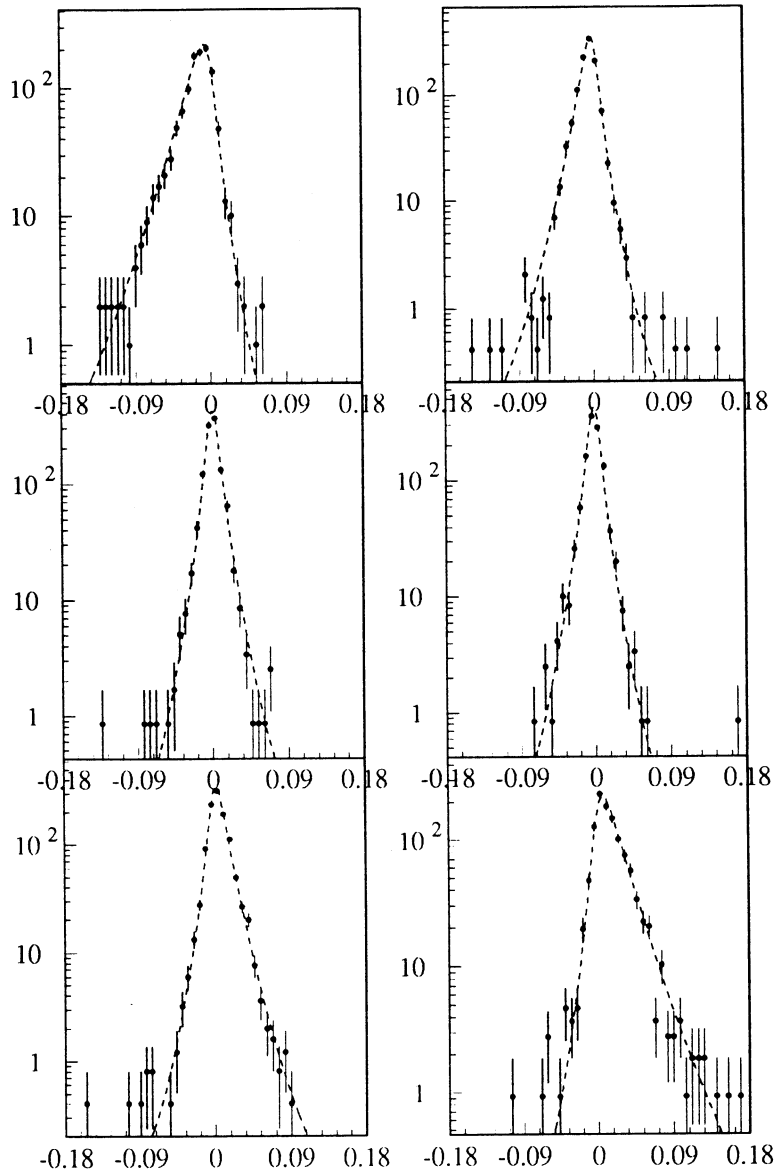

Figure 16: (a)–(e): δ distribution for various ranges of $S = \psi_1 + \psi_2$; (a) $S < -0.06$, (b) $-0.06 \leq S < -0.01$, (c) $-0.01 \leq S < 0.01$, (d) $0.01 \leq S < 0.06$, (e) $S \geq 0.06$. The solid line shows the fit result.

Table 9: systematic biases and uncertainties.

source	$\Delta\tau_\tau/\tau_\tau(\%)$	
Monte Carlo bias	-1.16	± 0.41
Background	-0.13	± 0.05
Branching Ratios & electron fraction mismatch (helix fit)	-0.12	± 0.28
τ transverse Polarization	-0.22	± 0.44
τ mass		± 0.03
Σd_0 resolution core: correction factors		± 0.35
Σd_0 resolution: beam smearing approximations		± 0.13
Σd_0 resolution tails within $10\sigma_g$: parametrization		± 0.22
Σd_0 resolution tails within $10\sigma_g$: MC accuracy		± 1.22
Σd_0 resolution tails beyond $10\sigma_g$: MC accuracy		± 0.30
Total	-1.63	± 1.49

The imperfection of the fitting procedure is corrected by comparing the Monte Carlo fit result for the decay length, $\ell = 0.2245 \pm 0.0009$ cm (99483 events), with the lifetime of the τ sample, 0.2271 cm. This corresponds to a bias of $(-1.16 \pm 0.41)\%$.

The following sources of background are considered: $Z \rightarrow q\bar{q}$, e^+e^-, and $\mu^+\mu^-$; $\gamma\gamma \rightarrow l^+l^-$ where l = e, μ, τ; $\gamma\gamma \rightarrow$ hadrons and cosmic rays. Their effect on the Monte Carlo fit result has been measured to determine the related bias and systematic error contribution, by varying each background estimate within its error (see table 3).

The τ branching ratios and the correlation of the τ^+ and τ^- transverse polarizations affect the angular and momentum distributions of undetected neutrinos, and therefore the precision on the measurement of the sphericity axis.

The τ branching ratios for the various one-prong modes have been varied within their errors [8]. The fraction of events containing one or more electrons is 0.368 ± 0.002 in Monte Carlo and 0.346 ± 0.005 in data; the discrepancy is primarily determined by the helix fit χ^2 cut, as discussed in [4]. The electron fraction in the Monte Carlo has been reduced to match the data, and the corresponding lifetime shift has been taken as systematic bias. This will account for the fact that the h function has been determined from Monte Carlo and is being used for the data as well. The branching ratios and the electron fraction discrepancy contribute therefore a total systematic bias of $(-0.12 \pm 0.28)\%$.

The correlation of the transverse polarization of the two τ leptons is not simulated in KORALZ [9]. This effect has been investigated by using 300,000 events produced by the KORALB Monte Carlo generator[3] [10]. The correlation of the transverse polarization correlates the decay angles of the two τ leptons in the $\tau - \varphi$ projection, therefore influencing the event axis error. Events are generated with and without the correlation. The fitted decay length is found to be $(0.22 \pm 0.44)\%$ smaller when the correlation is included.

The parametrization of the impact parameter sum resolution originates several systematic uncertainties. The gaussian core of the resolution has been tuned with real data events: the variation of the tuning coefficients within their statistical errors results in a per cent lifetime shift of 0.35%. The main source of systematics on the resolution tails arises from the estimated accuracy of the Monte Carlo simulation. As already seen, the resolution pull

[3]KORALB includes the effects due to the Z exchange process, but it is not appropriate for general studies as it lacks radiative corrections.

has been parametrized with a sum of three gaussians. The height of the second gaussian, the one that fits the non gaussian tails up to 10 times the gaussian core sigma, σ_g, is varied such that the R.M.S. width within $10\sigma_g$ changes by 4% of σ_g. The corresponding lifetime shift is 1.22%, which is the largest systematic contribution for the τ lifetime measurement. To account for the arbitrary parametrization that has been chosen for the resolution, the first two gaussians have been replaced by a single gaussian, preserving the overall R.M.S. width. One half of the lifetime shift is quoted as systematic error. Finally, the normalization and the sigma of the third gaussian, the one that fits the tails beyond $10\sigma_g$, are varied within 30% of their values, to take into account the Monte Carlo simulation accuracy once again.

The impact parameter sum distributions for data and Monte Carlo muons have a statistically significant average. A gaussian fit results in an average of $0.77 \pm 0.16\,\mu$m for Monte Carlo, and $2.10 \pm 0.25\,\mu$m for data. Statistically significant deviations from zero are only expected if detector misalignement cannot be reduced to a rigid roto-translation, but affects the track curvature. Monte Carlo and data τ pairs i.p. sum distributions have comparable averages. The consequent lifetime shift has been estimated by shifting the mean of the g resolution function by the averages found for the muons in data and Monte Carlo. It was found to be negligible.

Finally, a systematic contribution is added, to account for the approximations that have been done regarding the beam size smearing. The Monte Carlo lifetime shift resulting from the elimination of the beam smearing is quoted as systematic uncertainty.

The resulting systematic biases and uncertainties are summarized in table 9.

8 Conclusions

The τ mean lifetime has been measured by a maximum likelihood fit on the impact parameter sum distribution for $Z^0 \to \tau^+\tau^-$ events. The fit result, after subtraction of all the estimated biases, yields the following preliminary result:

$\tau_\tau = 295.0 \pm 3.9\,(\text{stat}) \pm 4.4\,(\text{syst})\,\text{fs}$

where $m_\tau = 1776.9 \pm 0.2 \pm 0.2\,\text{MeV/c}^2$ has been assumed [11].

References

[1] M. Carpinelli *et al.*, "Using the sum of impact parameters to measure the τ lifetime", ALEPH note 92-025, February 27, 1992.

[2] D. Decamp *et al.* (ALEPH Collaboration), Phys. Lett. B **279** (1992) 411.

[3] G. Ganis, M. Girone and G. Rolandi, "Improved $Z \to \tau^+\tau^-$ selection", ALEPH note 93-184, December 3, 1993.

[4] S. Wasserbaech, internal ALEPH note in preparation.

[5] K. Hikasa *et al.* (Particle Data Group), Phys. Rev. D **45** (1992) S1.

[6] D. Brown, M. Frank, "Tagging b hadrons using track impact parameters", ALEPH note 92-135, August 24, 1992.

[7] D. Brown, "QFNDIP, a primary vertex finder", ALEPH note 92-042, March 19, 1992.

[8] D. Decamp *et al.* (ALEPH Collaboration), Z. Phys. C **54** (1992) 211.

[9] Computer program **KORALZ**, version 3.4, courtesy of S. Jadach, B.F.L. Ward, and Z. Wąs; S. Jadach and Z. Wąs, Comp. Phys. Commun. **36** (1985) 191; Monte Carlo Group in "Proceedings of the Workshop on Z Physics at LEP," CERN Report 89-08 (1989) Vol. III; S. Jadach, B.F.L. Ward, and Z. Wąs, Comp. Phys. Commun. **66** (1991) 276.

[10] Computer program KORALB; S. Jadach and Z. Wąs, Comp. Phys. Commun. **64** (1991) 267.

[11] J.Z. Bai *et al.* (BES Collaboration), SLAC-PUB-5870 and BEPC-EP-92-01 (1992).